DAWN'S GAMMA RAY AND NEUTRON DETECTOR (GRAND)

ARCHIVE DESCRIPTION

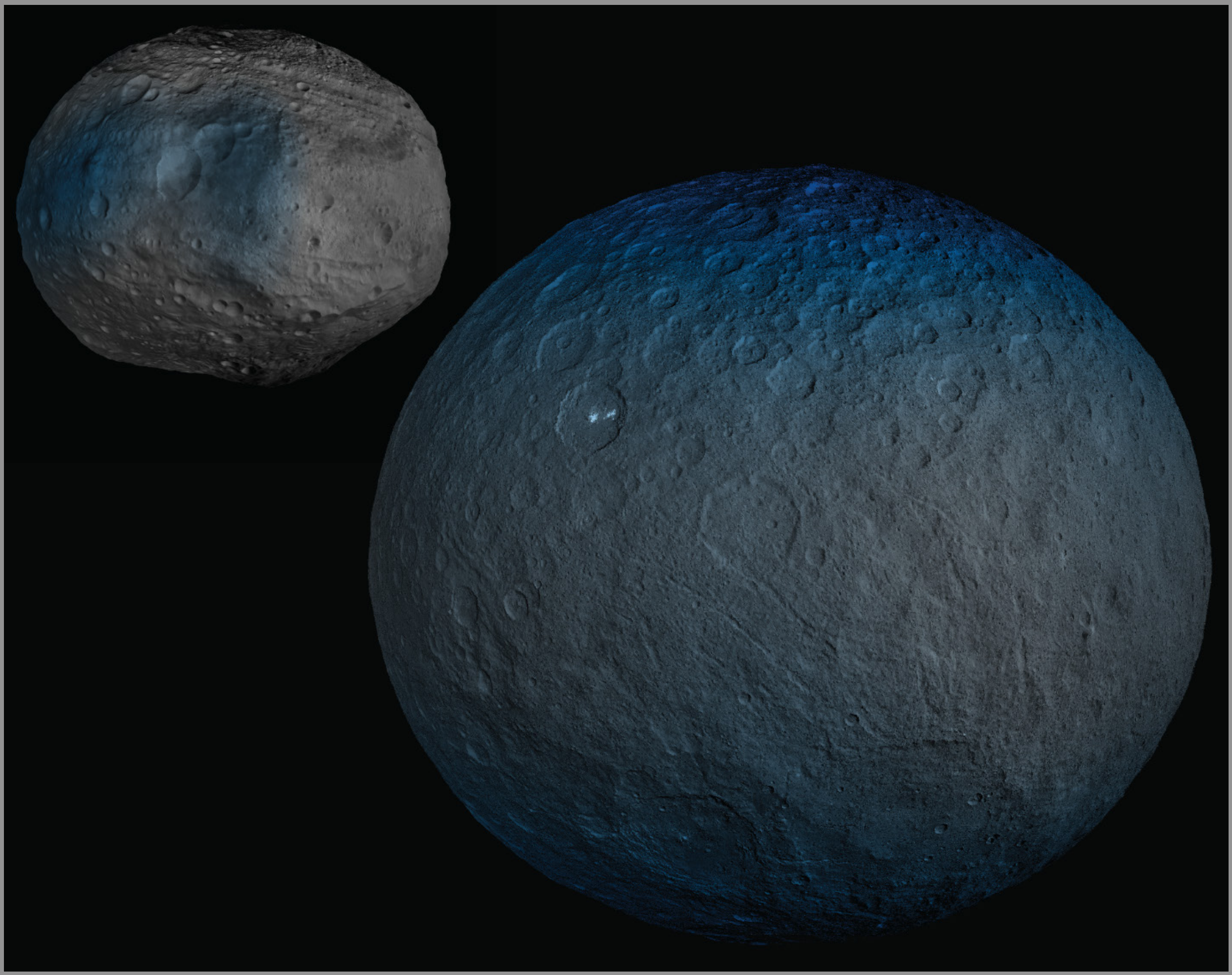

Version 1.0

Thomas H. Prettyman, Naoyuki Yamashita, Carol Neese, and Jesse Stone

Planetary Science Institute

8-Feb-2021

CONTENTS

ACRONYMS AND ABBREVIATIONS

ATLO	Assembly, Test, and Launch Operations
FC	Dawn Framing Camera
GRaND	Gamma Ray and Neutron Detector
HAMO	High altitude mapping orbit
LAMO	Low altitude mapping orbit
MCA	Mars Closest Approach
PDS	Planetary Data System
S/C	Spacecraft
SCLK	Spacecraft clock ticks (s), pronounced "S-clock"
SBN	PDS Small Bodies Node
TELREADOUT	Length of each science accumulation interval (s)
TELSOH	Sampling interval for the state of health telemetry (s)
VIR	Dawn Visible and Infrared Mapping Spectrometer
XML	eXtensible Markup Language

INTRODUCTION

***If you were wondering where to start, you have come to the right place*.** This document provides an introduction to the Dawn Gamma Ray and Neutron Detector (GRaND) Planetary Data System (PDS) archive, which is now compliant with the PDS4 standard. All the GRaND data from the Dawn mission were originally delivered in the now obsolete PDS3 format. Recently, NASA requested that the Dawn data be brought up to date. So, the PDS Small Bodies Node (SBN) and the GRaND team at the Planetary Science Institute worked together to create this new and improved archive.

What's are the new features of the archive? The data were migrated directly from PDS3 to PDS4. This process involved some reorganization of the archive along with the production of new labels and documentation. None of the data files have changed; however, a new data file has been added to provide a comprehensive list of live times and galactic cosmic ray (GCR) interaction rates, expanding on the existing compilation and correcting an error in the final mission phase. The main difference involves exciting new features enabled by PDS4, wherein the open-standard, eXtensible Markup Language (XML) is used to build labels with a rich set of metadata. XML provides more flexible and descriptive labeling of data files, allowing advances in software and database capabilities to be leveraged. The archive uses the nuclear spectroscopy (NucSpec) discipline dictionary developed by the SBN with input from the planetary community. NucSpec links data with instrument settings and parameters, enabling efficient identification of records for analysis. In addition, metadata is provided to identify solar energetic particle events and other phenomena of interest to the space and astrophysics communities. Software tools were developed for easy access and processing of raw data for scientific analyses (*dawn-grand-tools* archived at the NASA GitHub site. The new XML features and software tools are described.

***Significance*.** The NASA Dawn mission spent 11 years in flight, acquiring data during cruise through interplanetary space, observing Mars during a brief flyby, and measuring the elemental composition of Vesta and Ceres, the most massive bodies in the main asteroid belt. Chemical information was acquired by Dawn's Gamma Ray and Neutron Detector (GRaND), which measured radiation produced by galactic cosmic ray interactions with the outermost layers of the planetary targets [1-8]. GRaND also detected GCRs, solar energetic particles (SEPs), solar-flare X-rays and gamma-ray bursts (GRBs) [9,10]. Bursts of energetic electrons detected by GRaND while Dawn was in orbit around Ceres may have resulted from fast-Fermi acceleration of electrons at a bow shock formed by a transient atmosphere [10-13]. Data acquired by GRaND can be used for future studies on how solar energetic particles propagate through the heliosphere, important for both for science and understanding how space weather could impact upcoming planetary missions. Thus, the data acquired by GRaND crosses the boundaries of several disciplines within space science.

Changes in documentation. What happened to the Software Interface Specification (SIS)? Granted, the PDS3/SIS was an extremely useful document. It provided a general overview of the Dawn mission, introductory information about the instrument and data products, the organization of the data within the archive, and example PDS3 labels. We've replaced the SIS and catalog files with this and accompanying documents, which we hope will make the archive easier to use. To learn more, read on.

DAWN MISSION: GRAND PERSPECTIVE

The Dawn mission studied two main belt asteroids, Vesta and Ceres. Both bodies are believed to have accreted early in the history of the solar system. They were selected because they are thought to represent conditions and processes active early in the formation of the solar system. They developed into two characteristically different protoplanets. Vesta is a dry differentiated body shaped primarily by igneous processes. Ceres is a water-rich body that experience extensive aqueous alteration, with a regolith rich in hydrated minerals, carbon-bearing species and water ice. By studying both of these bodies, the Dawn mission compared the different evolutionary path each took and provided new insights into aspects of the early solar system.

To carry out its scientific mission, the Dawn spacecraft carried three science instruments. These instruments were: a visible camera (FC), a visible and infrared mapping spectrometer (VIR), and a gamma ray and neutron spectrometer (GRaND). In addition to these instruments, radiometric and optical navigation data provided data relating to the gravity field and thus bulk properties and internal structure of the two bodies.

The Dawn spacecraft was launched on September 27, 2007 on a Delta II 2925-9.5 Heavy from Cape Canaveral Air Force Station (Fig. 1). Using its ion propulsion subsystem Dawn departed for Vesta, flying by Mars in February 2009. The spacecraft arrived at Vesta on July 16, 2011, performed its orbital operations there, and departing on September 5, 2012. Dawn arrived at Ceres on March 5, 2015, where Dawn orbited until the end of the baseline mission (Fig. 1). The Dawn extended mission began July 1, 2016, with the spacecraft continuing its orbital operations at Ceres.

Dawn was an asteroid mapping mission. Each asteroid encounter was sub-divided into three mapping phases, each at different altitudes, and each with different science objectives and primary experiments. Shortly after orbit

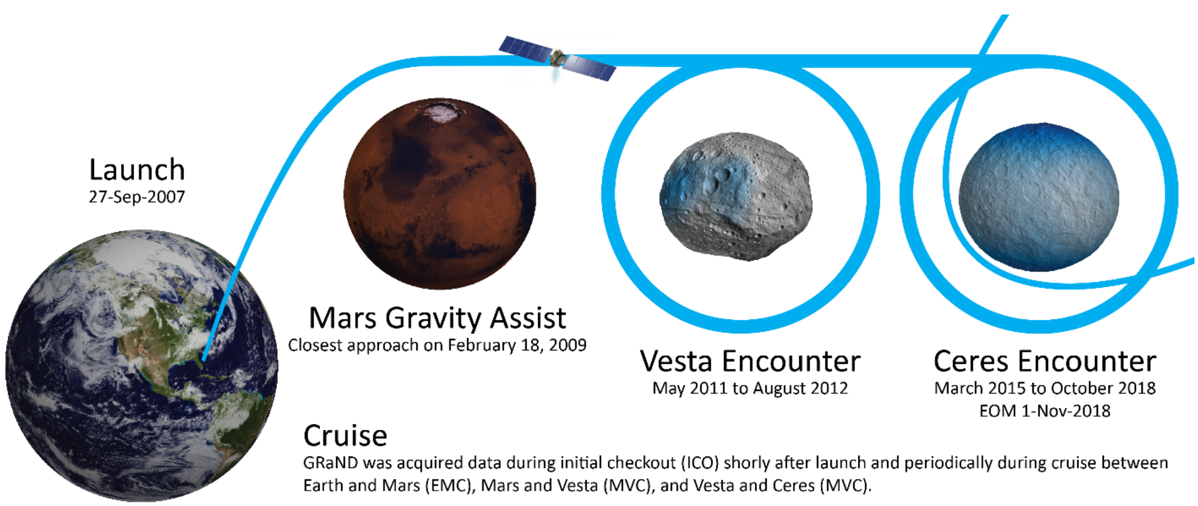

Figure 1. *Mission timeline*. Data were acquired by GRaND during Mars Gravity Assist and Vesta and Ceres orbital campaigns. Date ranges indicate periods of time when GRaND was operational. The spacecraft carrier signal was lost on 31-Oct-2018 while in the final, low-periapsis, eccentric orbit around Ceres; however, End of Mission (EOM) was not confirmed until the next day. The Vesta and Ceres images show the distribution of hydrogen (in blue) from [1,2]. *Credits*: Earth texture from the NASA Visible Earth/Blue Marble collection; Mars texture by Selden Ball of Cornell (derived from USGS Viking color mosaic); S/C image by NASA/JPL/Caltech.

capture the spacecraft entered a survey altitude mapping orbit where the VIR instrument was primary. This phase was relatively short, lasting for only 6-7 orbits. Global spectroscopy data and low-resolution global image mosaics were acquired during survey at each asteroid. After survey, the spacecraft was maneuvered into a high altitude mapping orbit (HAMO) where the FC instrument was primary. Medium resolution global stereo imaging was performed at this altitude (950 km Vesta, 1950 km Ceres) while local high-resolution spectroscopy data was acquired. Finally, the spacecraft proceeded to the low altitude mapping orbit (LAMO) where the GRaND and gravity experiments collected their prime data and additional, local, high resolution imaging and spectroscopy data were acquired. For Dawn's primary mission to Vesta and Ceres, the low altitude mapping orbits were approximately circular polar mapping orbits, approximately 0.8 body radii in altitude [8]. On asteroid approach, all the instruments performed in-flight calibrations and acquired data that were used to characterize the hazards of the near asteroid environment (dust) and search for moons.

Dawn's extended mission provided the opportunity to explore different data acquisition strategies. Notably, in the very last mission phase, Ceres X2 Elliptical (C2E), the spacecraft was placed in a highly eccentric orbit with periapsis that approached within 50 km of the surface. In this orbit, GRaND data were acquired with high elemental sensitivity and spatial resolution on the scale of geologic units [14]. The spacecraft delivered data for 123 of the eccentric orbits prior to End-of-Mission. Of these, 113 provided information useful for elemental analyses [14].

WHAT'S IN THE ARCHIVE?

OVERVIEW

The archive contains GRaND data acquired by the Dawn mission during its 11 years in flight. The processing levels include:

- **raw**: The raw data consist of time-ordered gamma-ray and neutron counting data, spectra, and housekeeping data acquired during each phase of the mission. The raw data were derived from spacecraft telemetry using reversible operations, providing a complete data set from which higher-level products can be derived. The time-series data are subdivided into coarse time intervals, roughly aligned with mission phase boundaries.
- **calibrated**: The calibrated data include a time series of gain-corrected BGO pulse height spectra as well as information about spacecraft location, pointing, and measurement geometry needed for quantitative analyses of elemental composition.
- **derived**: The derived data include maps of counting data and elemental abundances at Vesta and Ceres.

The data are coarsely subdivided into bundles for each of Dawn's primary mission targets and interplanetary cruise: **dawn-grand-mars**, **dawn-grand-vesta**, **dawn-grand-ceres**, and **dawn-grand-cruise**. Note that the target name for cruise was "calibration." An ancillary bundle (**dawn-grand-ancillary**) includes supplementary data, such as shape models used to derive geometry corrections, as well as key instrument settings and parameters.

The data acquired by GRaND is summarized in Table 1 and Fig. 2. Table 1 gives the number of science data records acquired by mission phase and target. The data volume for four different observing conditions tracked in the XML labels are also indicated. These include solar energetic particle (SEP) events, solar flare X-rays (SF), gamma-ray bursts (GRB), and data glitches.

The mission phases (phase IDs) with the highest data volume (indicated by the histogram in Table 1) are VESTA SCIENCE LAMO (VSL), CERES SCIENCE LAMO (CSL), CERES X2 HOLDING (CX2), and CERES X2 ELLIPTICAL (C2E). With the exception of CX2, these phases brought the spacecraft close to Vesta and Ceres and are the primary mission phases for the GRaND investigation. For the low altitude mapping orbits (LAMO), the spacecraft was about 0.8 body radii from Vesta and Ceres. The periapses of the highly eccentric orbits in C2E were within 50 km of the surface of Ceres. Close proximity and quiet Sun conditions (absence of events categorized under observing conditions) are required for high-sensitivity measurements of surface elemental composition using nuclear spectroscopy [15]. Nearly all the data in LAMO and in eccentric orbits at Ceres were acquired under quiet Sun conditions. The volume of data acquired under these conditions in LAMO at Vesta and Ceres is similar, despite that 35% of records at Vesta were acquired during solar energetic particle events. During the mission, GRaND acquired nearly a million science data records that can be used to determine the chemical makeup of Mars, Vesta and Ceres and to characterize the space environment in the main belt.

Table 1. GRaND data volume by Dawn mission phase. The table shows the number of science data records acquired by GRaND while fully configured for science data acquisition. The number of records assigned to different categories of observing conditions are listed (shown in red in the histogram). The influence of solar activity was minimal for the balance of records (shown in black).

					Records				
Start date	**Stop date**	**Mission phase name**	**Phase ID**	**Target**	**Total**	**SEP**	**SF**	**GRB**	**Glitch**
2007-10-16	2008-04-08	INITIAL CHECKOUT	ICO	Calibration	5658	0	0	0	0
2009-01-20	2009-01-22	EARTH-MARS CRUISE	EMC	Calibration	582	0	0	0	0
2009-01-22	2009-03-27	MARS GRAVITY ASSIST	MGA	Mars	19530	0	0	0	28
2009-11-30	2010-07-25	MARS-VESTA CRUISE	MVC	Calibration	4675	0	0	0	0
2011-05-03	2011-08-11	VESTA SCIENCE APPROACH	VSA	(4) Vesta	39282	10497	8	3	72
2011-08-11	2011-09-01	VESTA SCIENCE SURVEY	VSS	(4) Vesta	8640	813	0	0	8
2011-09-01	2011-10-06	VESTA TRANSFER TO HAMO	VTH	(4) Vesta	10240	0	32	5	2040
2011-10-06	2011-11-03	VESTA SCIENCE HAMO	VSH	(4) Vesta	11287	0	7	0	2848
2011-11-03	2011-12-15	VESTA TRANSFER TO LAMO	VTL	(4) Vesta	29932	1664	8	0	15
2011-12-15	2012-04-27	VESTA SCIENCE LAMO	VSL	(4) Vesta	147714	51460	0	13	88
2012-04-28	2012-06-16	VESTA TRANSFER TO HAMO 2	VT2	(4) Vesta	30040	0	8	5	22
2012-06-15	2012-07-25	VESTA SCIENCE HAMO 2	VH2	(4) Vesta	16002	1023	7	10	8
2012-07-25	2012-08-02	VESTA TRANSFER TO CERES	VTC	(4) Vesta	3154	3154	0	0	0
2012-12-10	2014-06-30	VESTA-CERES CRUISE	VCC	Calibration	8873	0	0	0	7
2015-03-13	2015-04-24	CERES SCIENCE APPROACH	CSA	(1) Ceres	17138	3806	14	8	55
2015-04-27	2015-05-09	CERES SCIENCE RC3	CSR	(1) Ceres	4599	3560	0	0	10
2015-05-09	2015-05-30	CERES TRANSFER TO SURVEY	CTS	(1) Ceres	8635	0	0	3	0
2015-05-30	2015-07-01	CERES SCIENCE SURVEY	CSS	(1) Ceres	13190	4107	0	5	4
2015-07-01	2015-08-17	CERES TRANSFER TO HAMO	CTH	(1) Ceres	16276	0	0	0	53
2015-08-17	2015-10-23	CERES SCIENCE HAMO	CSH	(1) Ceres	12894	0	0	3	39
2015-10-22	2015-12-16	CERES TRANSFER TO LAMO	CTL	(1) Ceres	23683	3703	8	0	30
2015-12-16	2016-06-22	CERES SCIENCE LAMO	CSL	(1) Ceres	116508	0	0	8	53
2016-06-22	2016-08-31	CERES EXTENDED LAMO	CXL	(1) Ceres	43199	0	0	11	29
2016-08-31	2016-10-05	CERES TRANSFER TO JULING	CTJ	(1) Ceres	14511	0	0	3	23
2016-10-05	2016-11-02	CERES EXTENDED JULING	CXJ	(1) Ceres	11512	0	0	0	0
2016-11-02	2016-12-14	CERES TRANSFER TO GRAND	CTG	(1) Ceres	17266	0	0	0	28
2016-12-14	2017-02-22	CERES EXTENDED GRAND	CXG	(1) Ceres	23725	0	0	11	30
2017-02-22	2017-04-24	CERES TRANSFER TO OPPOSITION	CTO	(1) Ceres	25152	0	0	8	44
2017-05-02	2017-07-05	CERES EXTENDED OPPOSITION	CXO	(1) Ceres	25867	0	0	6	29
2017-07-05	2018-04-18	CERES X2 HOLDING	CX2	(1) Ceres	117625	15100	49	34	160
2018-04-18	2018-05-16	CERES X2 TRANSFER TO INTERMEDIATE	CTI	(1) Ceres	11524	0	0	0	15
2018-05-16	2018-05-30	CERES X2 INTERMEDIATE	C2I	(1) Ceres	6784	0	0	0	7
2018-05-30	2018-10-26	CERES X2 ELLIPTICAL	C2E	(1) Ceres	64280	0	0	3	56
				Cruise total	19788	0	0	0	7
				Vesta total	296291	68611	70	36	5101
				Ceres total	574368	30276	71	103	665
				Dataset total	909977	98887	141	139	5801

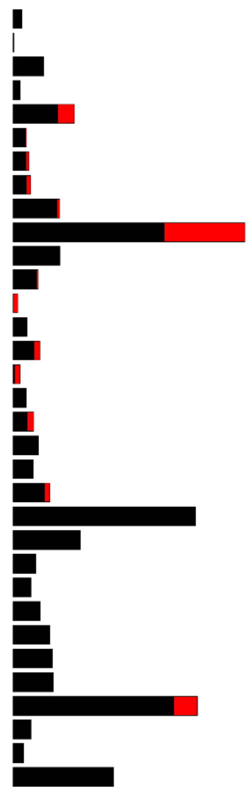

Histogram legend

Quiet Sun conditions

Observing condition active (SEP, SF, GRB, Glitch)

Figure 2 provides a graphical overview of the entire data set spanning 11 years of Dawn in flight. Selected signatures are displayed, including the live time fraction, gross interaction rate for the outboard scintillator (+Z phoswich), and the rate of three or more interactions ("triples"). See the documentation included in the archive for a description of the instrument and parameters. The live time fraction gives the fraction of each science accumulation interval for which the instrument was available to process radiation interactions. Accumulation of radiation damage effects and other changes in instrument performance likely contribute to the overall, gradual increase in the live time fraction during the mission. The live time fraction decreases with increasing interaction rate, which is highest when GRaND was in close proximity to Vesta (VSL) and Ceres (CSL and C2E) and during Mars encounter. The +Z phoswich scintillator is sensitive to solar energetic particles (SEP), which produce peaks in the time series. As demonstrated in Fig. 2, the triples monitor is sensitive to very high energy charged particles and serves as a proxy for the flux of galactic cosmic rays. GRaND's observations of solar and astrophysical phenomena while in the main belt supplement similar observations made at 1 A.U.

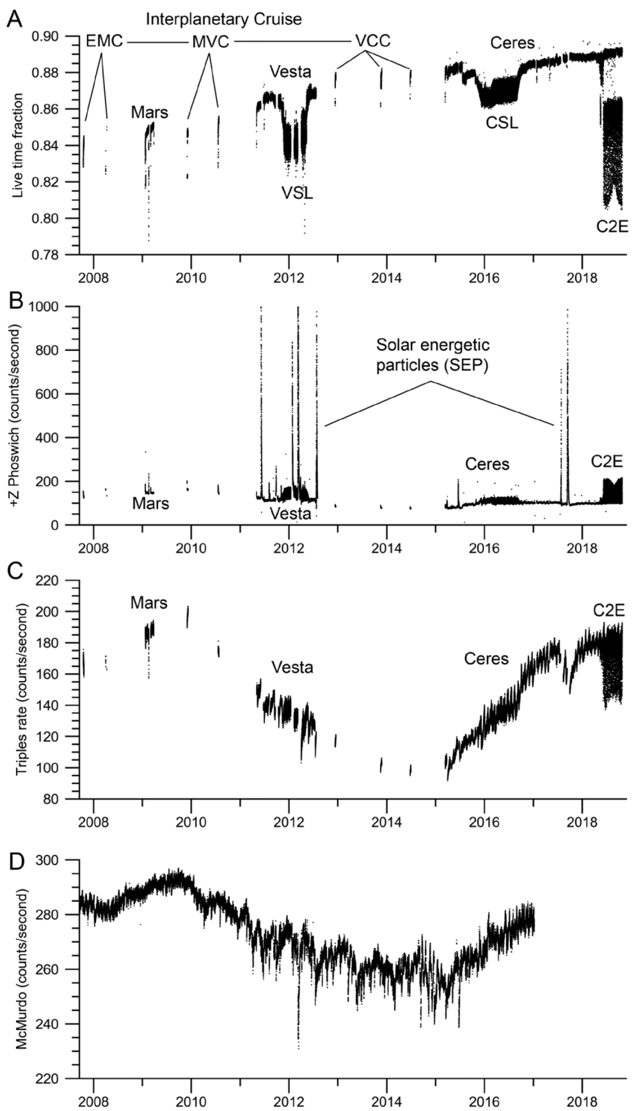

Figure 2. Overview of the dataset shows time series of GRaND science data products: **A**. The ratio of the live time of the counting system to the accumulation time. Live time varies inversely with the total interaction rate, which increases in proximity to planetary targets. **B**. The gross interaction rate for the +Z phoswich scintillator, which is sensitive to the passage of solar energetic particles (SEP). SEP events appear as peaks. **C**. The rate at which three or more sensors are struck. The triples rate is sensitive to minimally ionizing particles, primarily galactic cosmic rays. **D**. The count rate for the Bartol neutron monitors at McMurdo Station in Antarctica is also sensitive to galactic cosmic rays and shows a similar solar modulation trend to panel (Neutron monitors of the Bartol Research Institute are supported by the National Science Foundation). For visualization, SEP events were excluded from panels **A** and **C**. Mission phases indicated include Earth-Mars Cruise (EMC), Mars-Vesta Cruise (MVC), and Vesta Ceres Cruise (VCC). In Dawn's primary mission, the spacecraft's closest approach to Vesta and Ceres was about 0.8 body radii while in low altitude mapping orbit (VSL and CSL). The spacecraft approached within 50 km of the surface of Ceres while in a highly eccentric orbits during the final mission phase (C2E).

HOW TO GET STARTED

For users of the derived map data, the publications describing the maps are required reading (see data labels and bundle description documents). Map data can be read using the Interactive Data Language (IDL) with dawn-grand-tools available from GitHub and described in this document. Maps can be displayed in IDL and the data can be exported for use with other software packages (e.g., ENVI, ARCGIS).

For users wanting to reduce and analyze the data, essential reading includes the Space Science Review article describing GRaND [16] and documents in this bundle. These include the instrument description, raw and calibrated data documents, and supporting documents describing operations. The dawn-grand-tools IDL routines and PDS4 XML labels enable the user to remove (or identify) most records affected by solar and astrophysical phenomena, providing a clean data set that serves as a starting point for the analysis of planetary geochemistry. In addition to the migrated PDS3 data files and expanded metadata, we've added a comprehensive list of live times and triples rates in the dawn-grand-ancillary collection, which enables live-time corrections to be applied to all science data records for which GRaND was configured for science data acquisition.

Any user of the raw and/or calibrated time series data will need to match records across multiple data files. The spacecraft clock (SCLK) marking each science data record enables this. In the GRaND archive, all SCLK values are presented as long integers. Since the SCLK partitions did not change during the mission, the partition information is ignored. They are converted to strings for use with NAIF SPICE routines. The SCLK ticks accompanying each science data record marks the end of science accumulation interval. These are unique to each record and are used as a "serial code" to match records across files [17].

ARCHIVE CONTENTS

The PDS4 GRaND archive is made up of four bundles representing the data from the Mars flyby, the Vesta encounter, the Ceres encounter, and the Cruise phases, respectively, as well as an ancillary bundle containing information relevant to the archive as a whole. Each bundle contains a document collection, and except for the ancillary bundle, various data and browse collections.

Ancillary Bundle: This is where to get information about the GRaND instrument and the GRaND PDS4 archive. The bundle contains the following:

- document
  - ***Dawn GRaND archive*** (this document)
  - ***Instrument*** – Dawn_GRaND_instrument_description.pdf [18]
    Description of the instrument, including methods, science objectives, calibration, sensors, telemetry and accommodation on the spacecraft. Additional instrument details and flight performance through Mars Closest Approach can be found in [16].
  - ***Raw data*** - Dawn_GRaND_raw_data_description.pdf [19]
    Describes the raw data products found in the Cruise, Mars, Vesta and Ceres bundles. Helpful hint: When working with the raw data, it is useful to have a printout of Table 1 of [19] handy.
  - ***Ephemeris, pointing and geometry*** - Dawn_GRaND_ephemeris_pointing_geometry.pdf [17]
    Describes methods used to determine spacecraft position, pointing and measurement geometry (solid angles) at Vesta and Ceres. The document provides information relevant to all mission phases, such as how to match science data records across files, how to determine which housekeeping records belong to science accumulation intervals, scaler rollover corrections needed for determination of live time, and a description of temperature data found in SOH and EPG files.
  - ***Calibrated data processing*** - Dawn_GRaND_BGO_calibrated_data_processing.pdf [20]
    Describes methods used to reduce raw BGO single-interaction pulse height spectra to calibrated spectra for use in scientific studies. The calibrated time series spectra have been subjected to differential nonlinearity corrections, gain corrections and filtering of invalid records.
- miscellaneous

- *Instrument state table* – GRD_STATE_TABLE.TAB (Tables A1 and A2 of this document)
  Indexed table of instrument settings for which science data were acquired during the mission.
- *Live time table* – GRD_LIVETIME_TABLE.TAB (described in this document)
  Contains rollover-corrected live times and triples counting rates for records in all Dawn mission phases accumulated while the instrument was configured for science data acquisition.

Cruise Bundle: This contains just one data collection, ***data_raw***, as calibrated data were not produced for the cruise phases. It also contains a browse collection, and a document collection containing documents relating specifically to the cruise phases. See the Cruise Bundle Description in the Cruise bundle document collection for a detailed description of the contents of this bundle [21].

Mars Bundle: This contains two data collections, ***data_raw*** and ***data_calibrated***. It also contains a document collection with documents describing methods and operations specific to Mars Gravity Assist. This includes a separate Data Processing document that describes production of calibrated data and observational parameters used in the analysis of data acquired during Mars Flyby [22]. See the Mars Bundle Description in the Mars bundle document collection for a detailed description of the contents of this bundle [23].

Vesta Bundle: This contains three data collections, ***data_raw***, ***data_calibrated***, and ***data_derived***. The derived data are maps of counting data and elemental concentrations produced from the GRaND data by the Dawn Science Team. The browse collection contains browse products for the raw, calibrated, and derived data products. The document collection contains the Vesta Bundle Description [24], which provides a detailed description of the contents of this bundle and references to supporting information. In addition, there is a miscellaneous collection containing the Vesta shape model and PCK (SPICE kernel) used in the production of the calibrated and derived data.

Ceres Bundle: This contains three data collections, ***data_raw***, ***data_calibrated***, and ***data_derived***. The derived data are maps of counting data and elemental concentrations produced from the GRaND data by the Dawn Science Team. The browse collection contains browse products for the raw, calibrated, and derived data products. The document collection contains the Ceres Bundle Description [25], which provides a detailed description of the contents of this bundle and references to supporting information. In addition there is a miscellaneous collection containing the Ceres shape model used in the production of the calibrated and derived data.

FEATURES OF THE PDS4 ARCHIVE

The main feature of PDS4 is the use of the open-standard, eXtensible Markup Language (XML). XML provides more flexible and descriptive labeling of data files, allowing advances in software and database capabilities to be leveraged. The archive uses the nuclear spectroscopy (NucSpec) discipline dictionary developed by the Small Bodies Node (SBN) with input from the planetary community. NucSpec associates data with instrument settings and parameters, enabling efficient identification of records for analysis. Metadata is provided to identify solar energetic particles and other phenomena of interest to the space and astrophysics communities. In addition, the Dawn mission dictionary enables specification of keywords specific to GRaND, including the science accumulation interval (TELREADOUT) and the housekeeping telemetry sampling rate (TELSOH).

The structure of the XML files (schema) for the dictionaries used by the GRaND archive can be accessed via the following links:

- NucSpec discipline dictionary - https://pds.nasa.gov/datastandards/dictionaries/#nucspec
- Dawn mission dictionary - https://pds.nasa.gov/datastandards/dictionaries/#dawn

We note that while GRaND is the first user of the NucSpec dictionary, the dictionary was developed with future missions in mind. A subset of NucSpec features are used in the labels within this archive. They include matching records to selected instrument states and observing conditions. These features and their use in this archive are described here.

INSTRUMENT SETTINGS: STATE TABLE

Instrument settings include the configuration of subsystems, photomultiplier tube high voltages, and counting window parameters. At each target, these were held constant for as long as possible to ensure stable data acquisition; however, settings were occasionally adjusted to optimize instrument performance and to ensure that key signatures were on scale. Twenty-five operational states, for which the instrument was fully configured for science data acquisition, have been identified and recorded in the PDS4 labels; however, only a handful account for the bulk of the data volume (Fig. 3, Table 2, and Tables A1-2). The nil state (state index = 0) is recorded during instrument startup and shutdown or during anomaly resolution.

Users familiar with the PDS3 archive will recognize that inclusion of instrument settings in the label replaces much of the functionality of the state (-STA) files found in the raw collections [19]. The -STA files have been retained in the archive because they provide a complete list of instrument settings. Inclusion of the key operational settings in

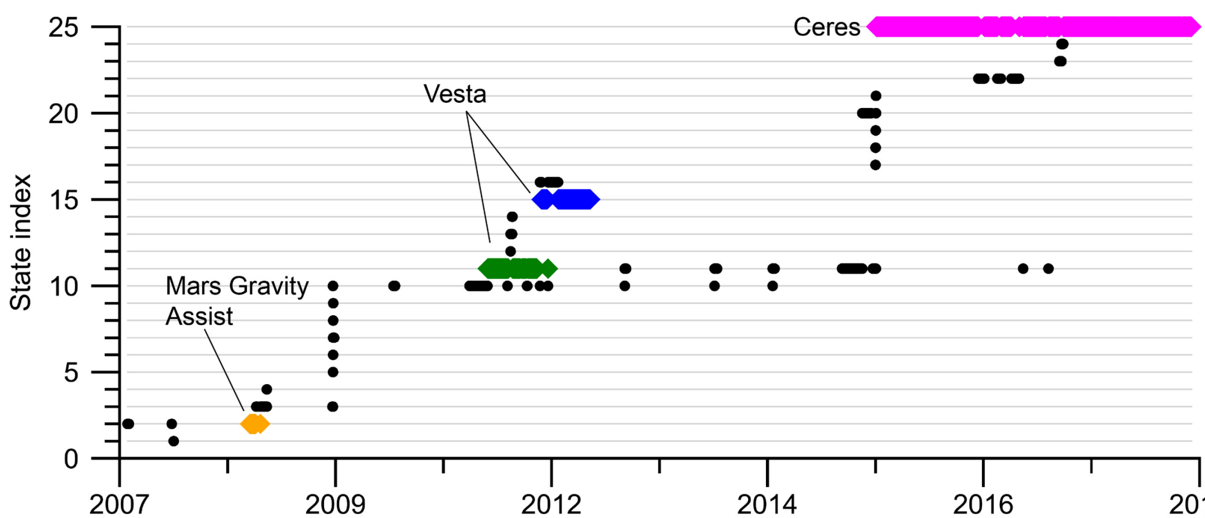

Figure 3. Graphical depiction of instrument settings. Primary states at Mars (2 - orange), Vesta (11 - green; 15 - blue), and Ceres (25 - magenta) are shown. Many of the other states are minor permutations on the primary settings used for testing and optimization of instrument parameters (see Table 2). For visualization, instances of nil states (state index = 0) are not shown.

the labels significantly enhances the archive, eliminating the tedious task of cross referencing time-series data in the raw and calibrated collections with information in the -STA files.

As indicated in Table 2, the instrument was configured in more than one way during Dawn's encounters with Mars, Vesta, and Ceres; although, the instrument settings were kept constant for long periods of time to ensure stable data acquisition. The settings tables in the Appendix (Tables A1 and A2) show that the differences between states are minor, and include gradual increases in high voltage to account for darkening of the scintillators due to the accrual of radiation damage and changes in coincidence window parameters. Minor changes include disabling of one of the Cadmium Zinc Telluride sensors (CZT9) starting with state 11 due to spurious behavior [16,26] and studies of changes in instrument parameters.

Table 2. Summary of the 26 instrument settings (states) recorded in the data labels. The table provides a brief description of each state. The nil state (index = 0) is assigned to records for which the instrument was not fully configured for science data acquisition (e.g., during startup, shutdown, or anomaly resolution). The number of raw data files in which each state appears is specified along with the number of affected data records and the phase identifiers for the mission phases in which they appear (see Table 1). Selected instrument states at Mars, Vesta and Ceres are color coded (orange, green, and magenta, respectively). Instrument settings for each state are given in the Appendix (Tables A1 and A2).

Ind.	Notes	Duration (days)	#files	#records	#phases	Phase IDs
0	Nil - A state index was not assigned.	-	80	1859	28	All
1	Same as 2 except for window settings	2.4	2	1000	2	ICO EMC
2	MGA through Mars Closest Approach (MCA)	30	17	18000	3	ICO EMC MGA
3	Post-MCA through MVC	31	10	14000	2	MVC MGA
4	Permutation/diagnostics/check-up	0.68	1	280	1	MGA
5	Permutation/diagnostics/check-up	0.16	1	67	1	MVC
6	Permutation/diagnostics/check-up	0.16	1	67	1	MVC
7	Permutation/diagnostics/check-up	3.9	2	1600	1	MVC
8	Permutation/diagnostics/check-up	0.16	1	67	1	MVC
9	Permutation/diagnostics/check-up	0.16	1	67	1	MVC
10	Initial settings at Vesta	71	19	30000	6	MVC VCC VSA VTH VTL VSL
11	Same as 10, but with an additional CZT channel disabled; initial setting during Ceres encounter	270	50	150000	13	CSA CSR CTS CTH CXG CXO VCC VSA VSS VTH VSH VTL VSL
12	CZT disabled	0.14	2	56	2	VTH VSH
13	CZT disabled	5.7	3	2300	2	VTH VSH
14	Permutation/diagnostics/check-up	1	1	420	1	VSH
15	Final settings at Vesta with increased +Z Phos. HV	150	26	110000	4	VSL VT2 VH2 VTC
16	Same HV settings as 10; window permutation	42	9	52000	1	VSL
17	Permutation/diagnostics/check-up	0.33	1	140	1	CTH
18	Permutation/diagnostics/check-up	0.33	1	140	1	CTH
19	Permutation/diagnostics/check-up	0.33	1	140	1	CTH
20	Primary setting for Ceres in CSS	34	8	14000	3	CTS CSS CTH
21	Permutation/diagnostics/check-up	0.33	1	140	1	CTH
22	Same as 25 except reduced BGO HV to increase energy range in search of Ni	63	12	31000	5	CXL CTJ CXJ CTG CXG
23	Permutation/diagnostics/check-up	7.8	2	3200	1	CXO
24	Permutation/diagnostics/check-up	6.8	2	2800	1	CXO
25	Primary setting for Ceres from CTH through EOM	1100	162	500000	15	CTH CSH CTL CSL CXL CTJ CXJ CTG CXG CTO CXO CX2 CTI C2I C2E

The NucSpec metadata appears under Processing_Information//NucSpec_Observational_Properties in all of the labels in the raw and calibrated collections except for the labels accompanying the -STA and -SCI-SOH data files. An example of the nil state (State index = 0), corresponding to instrument power on and configuration, which lasts over 250 minutes based on the SCLK entries, can be found in the very first raw data file in the cruise bundle, GRD-L1A-071016-071017_110225-SCI-SCL.xml. For the balance of the records in the file (about 170 minutes of data), the instrument settings are given by state index 2 (shown in Tables A1 and A2). Science data records within the SCLK ranges (start and stop times, inclusive) can be matched to the nil state and state index 2. The state table is defined using an Internal_Reference with a type of nucspec_product_to_state_table, and the index of the state table that matches the records is defined in State_Table_Entry. (The **$** signs in the examples indicate a line has been broken for visualization in this document).


```
<nucspec:Instrument_Settings>
  <nucspec:State_Table>
    <Internal_Reference>
      <lid_reference>urn:nasa:pds:dawn_grand:data:state_table</lid_reference>
      <reference_type>nucspec_product_to_state_table</reference_type>
    </Internal_Reference>
    <Local_Internal_Reference>
      <local_identifier_reference>table</local_identifier_reference>
      <local_reference_type>state_table_to_data_table</local_reference_type>
    </Local_Internal_Reference>
    <nucspec:State_Table_Entry>
      <nucspec:state_index xsi:nil="true"
            $ nilReason="missing"></nucspec:state_index>
      <nucspec:comment>This state not defined in state table. Refer to
            $ GRD-L1A-071016-071017_110225-STA.xml</nucspec:comment>
      <nucspec:State_Time>
        <nucspec:state_time_field_name>SCLK</nucspec:state_time_field_name>
        <nucspec:Time_Range_SCLK>
          <nucspec:sclk_start_time>245828267</nucspec:sclk_start_time>
          <nucspec:sclk_stop_time>245843489</nucspec:sclk_stop_time>
        </nucspec:Time_Range_SCLK>
      </nucspec:State_Time>
    </nucspec:State_Table_Entry>
    <nucspec:State_Table_Entry>
      <nucspec:state_index>2</nucspec:state_index>
      <nucspec:State_Time>
        <nucspec:state_time_field_name>SCLK</nucspec:state_time_field_name>
        <nucspec:Time_Range_SCLK>
          <nucspec:sclk_start_time>245843559</nucspec:sclk_start_time>
          <nucspec:sclk_stop_time>245853779</nucspec:sclk_stop_time>
        </nucspec:Time_Range_SCLK>
      </nucspec:State_Time>
    </nucspec:State_Table_Entry>
  </nucspec:State_Table>
</nucspec:Instrument_Settings>
```

OBSERVING CONDITIONS

Analysis of planetary surface composition using passive interrogation with galactic cosmic rays requires long integration times under steady, quiet Sun conditions. This requires identification and removal of transient events. The following event categories are included in the raw and calibrated time series labels via the NucSpec dictionary:

- **Solar Energetic Particles (SEP)**: These are energetic particles produced by coronal mass ejections. The label files record SEP events large enough to invalidate quiet Sun conditions. Electron bursts have been observed only once, during and immediately after an SEP event at Ceres. Their presence is indicated in the comment for the associated SEP.
- **Solar flare (SF)** - GRaND sensors respond to solar flare X-rays. The labels record solar flare X-rays identified by correlation with data from the NOAA Geostationary Operational Environmental Satellite (GOES). When available, the magnitude of the solar flare is included in the metadata.
- **Gamma-ray bursts (GRB)** - GRaND is sensitive to large gamma-ray bursts. These are identified by correlation with bursts detected by the Gamma-ray Burst Monitor (GBM) on board the Fermi Gamma-ray telescope (Yu et al., 2016). The GRB name and Fermi trigger time are included in the label entries.
- **Data glitch (DG)** - These include instrument glitches and anomalies well as unidentified blips, such as uncategorized solar flare X-rays or GRBs. Solar flare X-ray events and GRBs are fast transients that occur on timescales less than an accumulation interval and therefor make up a very small fraction of the total data volume. The glitch list includes a ~3 week period in which instrument performance was anomalous.

The observing conditions included in the archive build on the blip catalog of Yamashita et al. (2018). Additional events have been added and the glitch list has been expanded using an automated (Gaussian second derivative) peak detector. The number of records for each observing category is tallied for each mission phase in Table 1. In addition, every event included in the labels is listed in the Appendix (Tables A3-6). In the labels for raw and calibrated time-series data, the observing conditions follow the state information under Processing_Information // NucSpec_Observing_Properties // Instrument_Settings. An example snippet from GRD-L1A-170906-170913_190118-SCI-SCL.xml, a raw data file label in the dawn-grand-ceres bundle follows:

```
<nucspec:Observing_Conditions>
  <nucspec:condition_type>SEP</nucspec:condition_type>
  <nucspec:Observing_Condition>
    <nucspec:condition_active>false</nucspec:condition_active>
    <nucspec:Time_Range_SCLK>
      <nucspec:sclk_start_time>557928245</nucspec:sclk_start_time>
      <nucspec:sclk_stop_time>558338375</nucspec:sclk_stop_time>
    </nucspec:Time_Range_SCLK>
  </nucspec:Observing_Condition>
  <nucspec:Observing_Condition>
    <nucspec:condition_active>true</nucspec:condition_active>
    <nucspec:comment>SEP</nucspec:comment>
    <nucspec:Time_Range_SCLK>
      <nucspec:sclk_start_time>558338585</nucspec:sclk_start_time>
      <nucspec:sclk_stop_time>558536405</nucspec:sclk_stop_time>
    </nucspec:Time_Range_SCLK>
  </nucspec:Observing_Condition>
          …
```

The example records a solar energetic particle event. The dictionary requires that the observing conditions for the entire time period covered by records within a file be defined. Consequently, the time period for which the SEP is not active is also indicated with condition_active = false. The same label identifies several solar flares. The time periods before, in between, and after the flares have entries with condition_active = false.

DAWN DICTIONARY: TELREADOUT AND TELSOH

The Dawn dictionary, which contains metadata relevant to each of Dawn's instruments, is used to specify the accumulation time for science data records and the housekeeping sampling time for GRaND. Users of the PDS3 archive will recognize that this information is also in the -STA files in each raw data directory. Organizing the information in the labels further reduces the effort required to reduce and analyze the data. As with the NucSpec library, all time ranges must be accounted for in the label. An example label snippet from the last raw data downlinked by Dawn at Ceres, GRD-L1A-181024-181026_181102-SCI-SCL.xml in the 20_CERES_X2_ELLIPTICAL directory, shows an example of multiple TELREADOUT entries (switching between 455s and 35s). The nil entry corresponds to the instrument being commanded to the 35s setting. During this time, TELREADOUT=2000s. The user is referred to the appropriate -STA file for further information.

```
 <dawn:grand>
   <Local_Internal_Reference>
     <local_identifier_reference>table</local_identifier_reference>
     <local_reference_type>grand_parameters_to_table</local_reference_type>
   </Local_Internal_Reference>
   <dawn:TELREADOUT_List>
     <dawn:TELREADOUT>
       <dawn:grand_start_sclk>593611574</dawn:grand_start_sclk>
       <dawn:grand_stop_sclk>593670724</dawn:grand_stop_sclk>
       <dawn:grand_interval unit="s">455</dawn:grand_interval>
     </dawn:TELREADOUT>
     <dawn:TELREADOUT>
       <dawn:grand_start_sclk>593670942</dawn:grand_start_sclk>
       <dawn:grand_stop_sclk>593670977</dawn:grand_stop_sclk>
       <dawn:grand_interval unit="s" xsi:nil="true"
              $ nilReason="missing"></dawn:grand_interval>
       <dawn:comment>This state not defined in state table. Refer to
              $ GRD-L1A-181024-181026_181102-STA.xml</dawn:comment>
     </dawn:TELREADOUT>
     <dawn:TELREADOUT>
       <dawn:grand_start_sclk>593671012</dawn:grand_start_sclk>
       <dawn:grand_stop_sclk>593683437</dawn:grand_stop_sclk>
       <dawn:grand_interval unit="s">35</dawn:grand_interval>
     </dawn:TELREADOUT>
             …
   <dawn:TELREADOUT_List>
</dawn:grand>
```

SOFTWARE TOOLS

Software is provided for easy access and processing of GRaND data for scientific analyses: dawn-grand-toolbox at the NASA GitHub site: https://github.com/nasa/dawn-grand-toolbox. The repository includes sample labels for evaluation. The software was written in the Interactive Data Language (IDL) and uses the xml_parse() function introduced in IDL 8.6.1. The GRaND archive only contains character and binary tables. Two routines are provided to ingest the data:

- **grd4_read_character_table** - IDL function that reads character (ASCII) tables, including most raw files and *all* calibrated and derived data files.
- **grd4_read_binary_table** - IDL function that reads binary data found in the raw data files containing time-series event mode gamma and neutron data.

The routines parse the label, extracting metadata useful for analysis, and read the data. For time series data files (raw and calibrated), the metadata includes mission phase and target information, instrument settings (STATE, TELREADOUT, and TELSOH) and observing conditions.

In addition to IDL tools specific to this archive, the PDS offers the generic PDS4 viewer, which can be used to examine the labels in a human-readable format: http://sbndev.astro.umd.edu/wiki/PDS4_Viewer. The Python tools that used to create the PDS4 viewer are available from PDS. For Python users, the IDL to Python bridge also enables interaction with the Python interpreter from IDL.

EXAMPLES

The following examples assume the user's current directory in IDL is set to the root directory containing the bundle directories and that the path separator is a backslash (\).

```
To select read a file interactively:

g = grd4_read_character_table()  ; a dialog box enables selection of the label file
help, g

If GRD-L1B-110505-110810_140930-VSA-BGOC.xml is selected, IDL prints:
** Structure <ccda1260>, 13 tags, length=137436168, data length=137303481, refs=1:
   FLAG             BOOLEAN    true (1)
   TARGET_NAME      STRING     '(4) Vesta'
   MISSION_PHASE_NAME
                    STRING     'VESTA SCIENCE APPROACH'
   MISSION_PHASE_IDENTIFIER
                    STRING     'VSA'
   SCLK_START       LONG          357845426
   SCLK_STOP        LONG          366292835
   STATE            LONG       Array[33165]
   TELREADOUT       LONG       Array[33165]
   TELSOH           LONG       Array[33165]
   OBSCON           STRUCT     -> <Anonymous> Array[1]
   RECORDS          STRUCT     -> <Anonymous> Array[33165]
   FORMAT           STRING     '(i10,a20,f12.1,1024i6)'
   FORMATC          STRING     '(%"%10d%20s%12.1f",1024(%"%6d"))'
```

```
To print the state table:

g = grd4_read_character_table(label='.\dawn-grand-ancillary\grd_state_table.xml')
print, tag_names(g.records)
print, g.records, format=g.format

IDL prints (output truncated for display):

STATE_INDEX MODE HVPS1_SET HVPS1 HVPS2_SET HVPS2 HVPS3_SET HVPS3 HVPS4_SET HVPS4
HVPS5_SET HVPS5 HVPS6_SET HVPS6 PM5_LVPS P12_LVPS CZT_PM5_LVPS CZT_ENABLES
NEMG_TOT_EVTS NEMG_CZT_EVTS NEMN_TOT_EVTS L_BGO_CW H_BGO_CW L_BGO_ROI
H_BGO_ROI L_BLP_MY_CW H_BLP_MY_CW L_BLP_MY_ROI H_BLP_MY_ROI L_BLP_PY_CW H_BLP_PY_CW
L_BLP_PY_ROI H_BLP_PY_ROI L_BLP_MZ_CW H_BLP_MZ_CW L_BLP_MZ_ROI H_BLP_MZ_ROI
L_BLP_PZ_CW H_BLP_PZ_CW L_BLP_PZ_ROI H_BLP_PZ_ROI
  1 1  1058.82 1  1000.00 1  1029.41 1  1058.82 1   735.29 1  1000.00 …
  2 1  1058.82 1  1000.00 1  1029.41 1  1058.82 1   735.29 1  1000.00 …
  3 1  1058.82 1  1000.00 1  1029.41 1  1058.82 1   735.29 1  1000.00 …
  4 1  1058.82 1  1000.00 1  1029.41 1  1088.24 1   735.29 1  1000.00 …
  5 1  1058.82 1  1000.00 1  1029.41 1  1058.82 1   735.29 1  1000.00 …
  6 1  1058.82 1  1000.00 1  1029.41 1  1058.82 1   735.29 1  1000.00 …
  7 1  1058.82 1  1000.00 1  1029.41 1  1058.82 1   735.29 1  1000.00 …
  8 1  1058.82 1  1000.00 1  1029.41 1  1088.24 1   735.29 1  1000.00 …
  9 1  1058.82 1  1000.00 1  1029.41 1  1117.65 1   735.29 1  1000.00 …
 10 1  1058.82 1  1000.00 1  1029.41 1  1058.82 1   735.29 1  1000.00 …
 11 1  1058.82 1  1000.00 1  1029.41 1  1058.82 1   735.29 1  1000.00 …
 12 1  1058.82 1  1000.00 1  1029.41 1   588.24 1   735.29 1     0.00 …
 13 1  1058.82 1  1000.00 1  1029.41 1  1058.82 1   735.29 1     0.00 …
 14 1  1058.82 1  1000.00 1  1029.41 1  1058.82 1   735.29 1   294.12 …
 15 1  1088.24 1  1000.00 1  1029.41 1  1058.82 1   735.29 1  1000.00 …
 16 1  1058.82 1  1000.00 1  1029.41 1  1058.82 1   735.29 1  1000.00 …
 17 1  1058.82 1  1000.00 1  1029.41 1  1058.82 1   700.00 1  1000.00 …
 18 1  1058.82 1  1000.00 1  1029.41 1  1058.82 1   711.76 1  1000.00 …
 19 1  1058.82 1  1000.00 1  1029.41 1  1058.82 1   723.53 1  1000.00 …
 20 1  1058.82 1  1000.00 1  1029.41 1  1058.82 1   747.06 1  1000.00 …
 21 1  1058.82 1  1000.00 1  1029.41 1  1058.82 1   752.94 1  1000.00 …
 22 1  1088.24 1  1017.65 1  1047.06 1  1070.59 1   723.53 1  1000.00 …
 23 1  1088.24 1  1017.65 1  1047.06 1  1070.59 1   711.76 1  1000.00 …
 24 1  1088.24 1  1017.65 1  1047.06 1  1070.59 1   700.00 1  1000.00 …
 25 1  1088.24 1  1017.65 1  1047.06 1  1070.59 1   747.06 1  1000.00 …
```

To illustrate how the the observing conditions metadata are used, we examine raw time series data that record a gamma-ray burst, solar flare X-ray events, and solar energetic particles. The data are found in the dawn-grand-ceres bundle, raw collection in the 16_Ceres_X2_HOLDING directory: GRD-L1A-170906-170913_190118

The +Z phoswich scintillator (PHOS_PZ) in the neutron subdirectory is sensitive to energetic particles, solar flare X-rays and gamma-ray bursts. The file can be selected and read via:

```
dir='.\dawn-grand-ceres\data_raw\16_CERES_X2_HOLDING\'
file='GRD-L1A-170906-170913_190118\neutron\GRD-L1A-170906-170913_190118-PHOS_PZ.xml'
g=grd4_read_character_table(label=dir+file)
```

The output contains a structure called records, which contains a time series of 256-channel pulse height spectra (g.records.phos_pz). The output also includes a structure called OBSCON, which contains the observing conditions, including a gamma-ray burst, five solar flare X-ray events, and a solar energetic particle event:

```
help, g.obscon, /str

IDL prints:
** Structure <cc019550>, 17 tags, length=11784, data length=11760, refs=2:
   ACTIVE_SEP       BOOLEAN   true (1)
   SCLK_START_SEP   LONG      Array[1]
   SCLK_STOP_SEP    LONG      Array[1]
   DESC_SEP         STRING    Array[1]
   FLAG_SEP         BOOLEAN   Array[2897]
   ACTIVE_SFLARE    BOOLEAN   true (1)
   SCLK_START_SFLARE
                    LONG      Array[5]
   SCLK_STOP_SFLARE
                    LONG      Array[5]
   DESC_SFLARE      STRING    Array[5]
   FLAG_SFLARE      BOOLEAN   Array[2897]
   ACTIVE_GRB       BOOLEAN   true (1)
   SCLK_START_GRB   LONG      Array[1]
   SCLK_STOP_GRB    LONG      Array[1]
   DESC_GRB         STRING    Array[1]
   FLAG_GRB         BOOLEAN   Array[2897]
   ACTIVE_GLITCH    BOOLEAN   false (0)
   FLAG_GLITCH      BOOLEAN   Array[2897]
```

The information in the OBSCON and RECORDS structures can be used to mark the observed events in a plot of the total phos_pz counts (Fig. 4). For example, the obscon.flag_sflare or obscon.sclk_start_sflare & sclk_stop_sflare can be used to mark records corresponding to solar flares. The following code can be used to generate the plot shown in Fig. 4:

```
phos_pz=total(g.records.phos_pz,1)
w=window(dimensions=[1000,800])& p=objarr(4)
p[0]=plot(g.records.sclk,phos_pz,axis_style=1,yrange=[0,1e5],/current)
p[0].xtickdir=1 & p[0].ytickdir=1 & p[0].xtickfont_size=16 & p[0].ytickfont_size=16
p[0].xtitle='SCLK (s)' & p[0].ytitle='Counts'
id=where(g.obscon.flag_sep)
p[1]=plot(g.records[id].sclk,phos_pz[id],symbol='o', sym_size=0.3, $
          sym_filled=1,linestyle=6,color='red',/over)
id=where(g.obscon.flag_sflare)
p[2]=plot(g.records[id].sclk,phos_pz[id],symbol='o', sym_size=0.5, $
          sym_filled=1,linestyle=6,color='blue',/over)
id=where(g.obscon.flag_grb)
p[3]=plot(g.records[id].sclk,phos_pz[id],symbol='o', sym_size=0.5, $
          sym_filled=1,linestyle=6,color='magenta',/over)
w.save, "<your graphics save dir>\observing_conditions_marked.png"
```

The figure can be improved by plotting count rates as a function of calendar date, which is enabled by the Julian dates and live times provided in the new GRD_LIVETIME_TABLE described in the next section. Count rates can be used to determine particle fluxes given measurement geometry and detection efficiency. The improved plot can be made by continuing the example above with the following fragment of code:

```
h=grd4_read_character_table(label=".\dawn-grand-ancillary\GRD_LIVETIME_TABLE.xml")
match, g.records.sclk, h.records.sclk, ig, ih
jul_mid=h.records[ih].jul_mid
phos_pz_rate=phos_pz/h.records[ih].live_time

w=window(dimensions=[1000,800])
p=objarr(4)
p[0]=plot(jul_mid,phos_pz_rate,axis_style=1,yrange=[0,1000],/current)
p[0].xtickdir=1 & p[0].ytickdir=1 & p[0].xtickfont_size=16 & p[0].ytickfont_size=16
p[0].xtitle='September 2017' & p[0].ytitle='Counts/second'
p[0].xtickformat='(C(CDI))' & p[0].xtickunits='Days' & p[0].xminor=1
id=where(g.obscon.flag_sep)
p[1]=plot(jul_mid[id],phos_pz_rate[id],symbol='o', sym_size=0.3, $
          sym_filled=1,linestyle=6,color='red',/over)
id=where(g.obscon.flag_sflare)
p[2]=plot(jul_mid[id],phos_pz_rate[id],symbol='o', sym_size=0.5, $
          sym_filled=1,linestyle=6,color='blue',/over)
id=where(g.obscon.flag_grb
p[3]=plot(jul_mid[id],phos_pz_rate[id],symbol='o', sym_size=0.5, $
          sym_filled=1,linestyle=6,color='magenta',/over)
w.save, "<your graphics save dir>\observing conditions marked.png"
```

The example makes use of the *match* function from the IDL Astronomy Users Library (http://idlastro.gsfc.nasa.gov) to determine which records in ***g*** match those in ***h*** by matching SCLK entries. The example also uses IDL's date formatting feature to convert Julian dates to days on the x-axis. We've cut corners by simply entering "September 2017" for the x-axis title rather than providing additional horizontal axes for the month and year. Converting Julian dates to calendar dates can be accomplished, for example, via:

```
print, jul_mid[0], format='(C(CDI,1x,CMoA,1x,CYI))'

IDL prints:
6 Sep 2017

print, jul_mid[-1], format='(C(CDI,1x,CMoA,1x,CYI))'

IDL prints:
13 Sep 2017
```

Users could alternatively obtain the Julian dates using SPICE routines and kernels from the Navigation and Ancillary Information Facility (NAIF). A leap seconds kernel and the Dawn SCLK kernel would be required to convert SCLK to Julian date; however, they would still need to read in the live times from GRD_LIVETIME_TABLE to determine interaction rates.

For the improved plot shown in Fig. 5, we've added in the GOES 15 X-ray fluxes[†] to show the correspondence between solar flare activity and the GRaND data. The data provide the timing of the arrival of solar energetic particles relative coronal mass ejections, which follow solar flares. Applications of the data include better understanding the propagation of solar energic particles beyond Earth's orbit needed for space weather predictions in the main belt.

†GOES N Data Book, prepared for NASA by Boeing, PM-1.1-03 Rev B, February 2005: https://www.nasa.gov/pdf/148080main_GOES-N%20Databook%20with%20Copyright.pdf

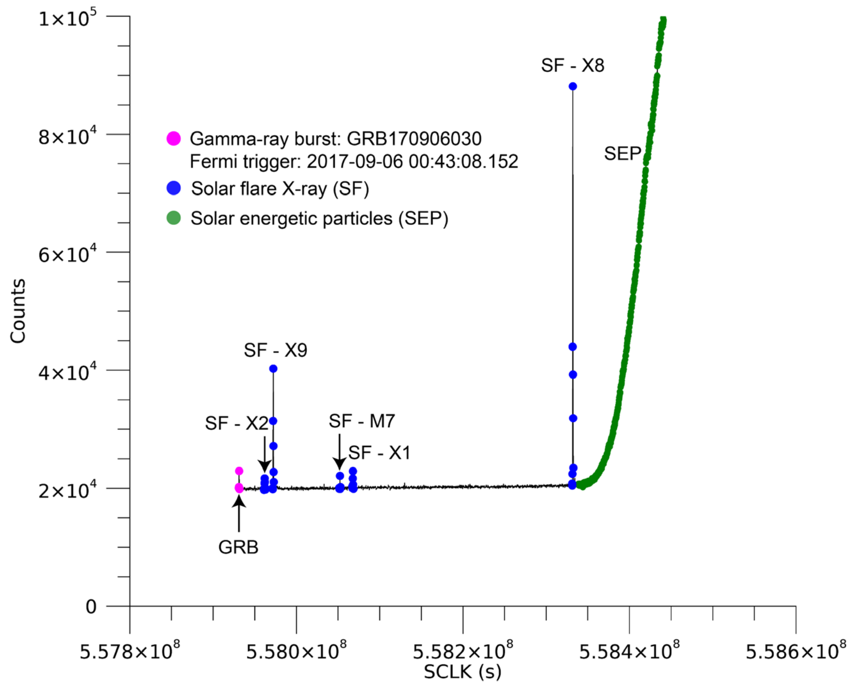

Figure 4. Time series of gross counts measured by the +Z phoswich scintillator during a period of intense solar activity. Events listed in the XML label file accompanying the data are marked. These include a gamma-ray burst (GRB), solar flare X-rays (SF), and solar energetic particles (SEP). The annotations are based on the information provided in the OBSCON structure (DESC_SEP, DESC_SF, and DESC_GRB).

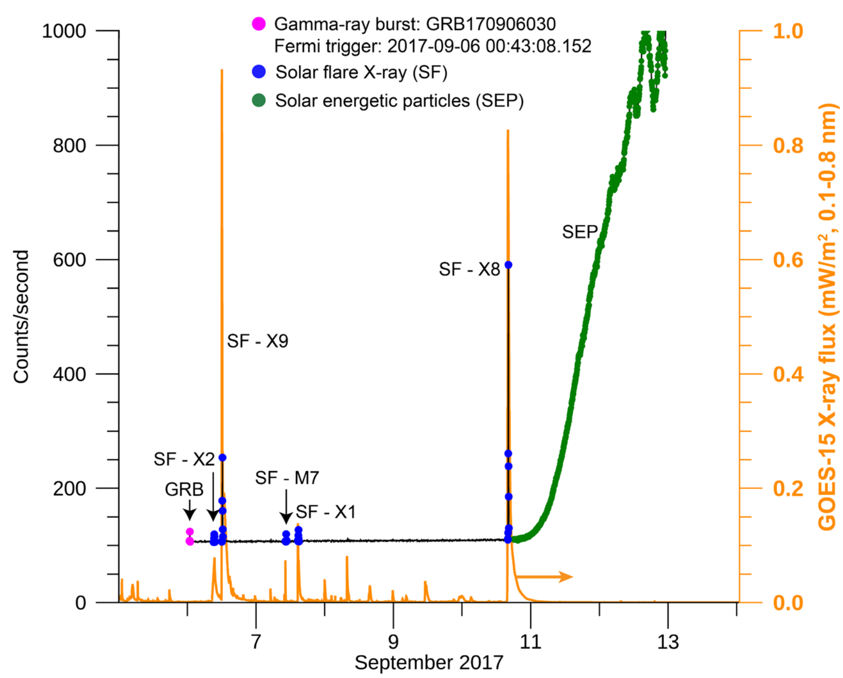

Figure 5. The data from Fig. 4 have been replotted as count rates and with the date range on the x-axis using information from GRD_LIVETIME_TABLE. We've also plotted GOES-15 X-ray fluxes (orange trace, right axis) to relate GRaND data and solar flare activity observed by GOES.

The derived bundles for Vesta and Ceres contain maps. These are tables that list map values for pixels defined by minimum and maximum latitudes and longitudes. Writing *efficient* code to create a map image from the table that can be plotted with different map projections is not a simple task for neophyte IDL users. Users can cut and paste the following snippet into the command line to read and plot maps. The code makes use of the *reverse indices* feature of the *histogram* function to carry out the task quickly no matter how long the list of input pixels. The example reads a hydrogen map from the Ceres derived bundle and creates a 720 × 360 image (variable name *map*) representing a 0.5 degree equirectangular map of the data. The map is displayed using the IDL *image* function with a Mollweide projection with the prime meridian on the left. The resulting map can be compared to the map displayed in the browse collection (dawn-grand-ceres\browse\derived\GRD_HYDROGEN_MAP.pdf).

```
g=grd4_read_character_table(label='.\dawn-grand-ceres\data_derived\GRD_HYDROGEN_MAP.xml')

unit=make_array(720,360,value=1,/float)
lonv=-179.75+findgen(720)/2 & lons=diag_matrix(lonv) # unit
hlons=histogram(lons,nbins=720,reverse_indices=rlon)
latv=-89.75+findgen(360)/2 & lats=unit # diag_matrix(latv)

map=fltarr(720,360)
for i=0L,g.records.length-1 do begin & $
  ilon=where(lonv gt g.records[i].min_lon and lonv lt g.records[i].max_lon, countl) & $
  rr=0L & for j=0L,countl-1 do rr=[rr,rlon[rlon[ilon[j]]:rlon[ilon[j]+1]-1]] & rr=rr[1:-1] & $
  id=where(lats[rr] gt g.records[i].min_lat and lats[rr] lt g.records[i].max_lat)   & $
  map[rr[id]]=g.records[i].h_conc & $
endfor

imap=image(map, grid_units=2, image_location=[-180,-90], center_longitude=-180, $
             image_dimensions=[360,180], map_projection='Mollweide', rgb_table=72)
```

IDL displays:

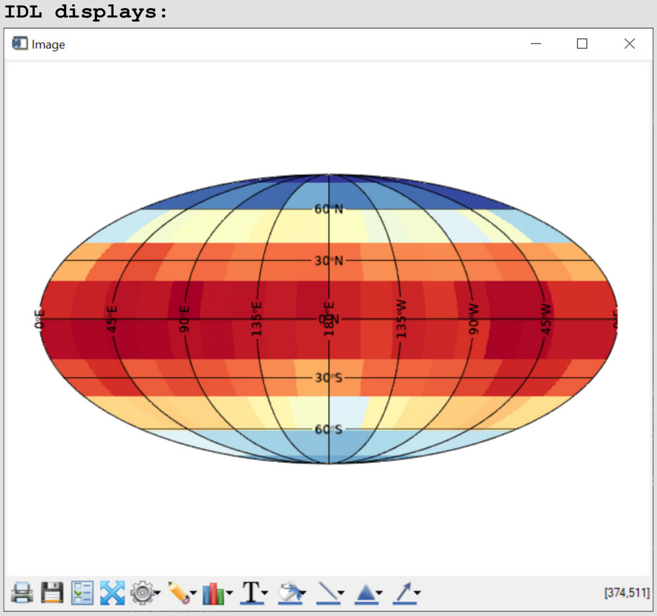

UPDATES: LIVE TIMES AND GALACTIC COSMIC RAY PROXY

In order to make the data set more accessible to users, we added a new file to the ancillary bundle (GRD_LIVETIME_TABLE) that contains a list of live times and rates for three or more interactions with GRaND for the entire mission. The latter is the so-called "triples" rate and is a proxy for galactic cosmic rays, many of which are minimally ionizing particles that can punch through the instrument, triggering the response of multiple sensors. The ephemeris, pointing and geometry (EPG) files in the calibrated bundles for Vesta and Ceres already contain these parameters; however, we wanted to provide a comprehensive, uniform list of values with associated SCLK ticks as well as epoch times, UTC and julian spacecraft event times. In the process, we discovered an error in the triples rates reported in the C2E mission phase when TELREADOUT was set to 455- and 910-seconds. In this condition, the triples scaler roll over was not correctly accounted for, resulting in discontinuities in corrected rates (Fig. 6). The new data file contains properly corrected triples rates. The EPG file was not modified in this release of the archive. Consequently, studies using the position and pointing information in the EPG file for the C2E mission phase, need to make live time and cosmic ray corrections using the information in GRD_LIVETIME_TABLE.TAB. The EPG file will be updated in future releases.

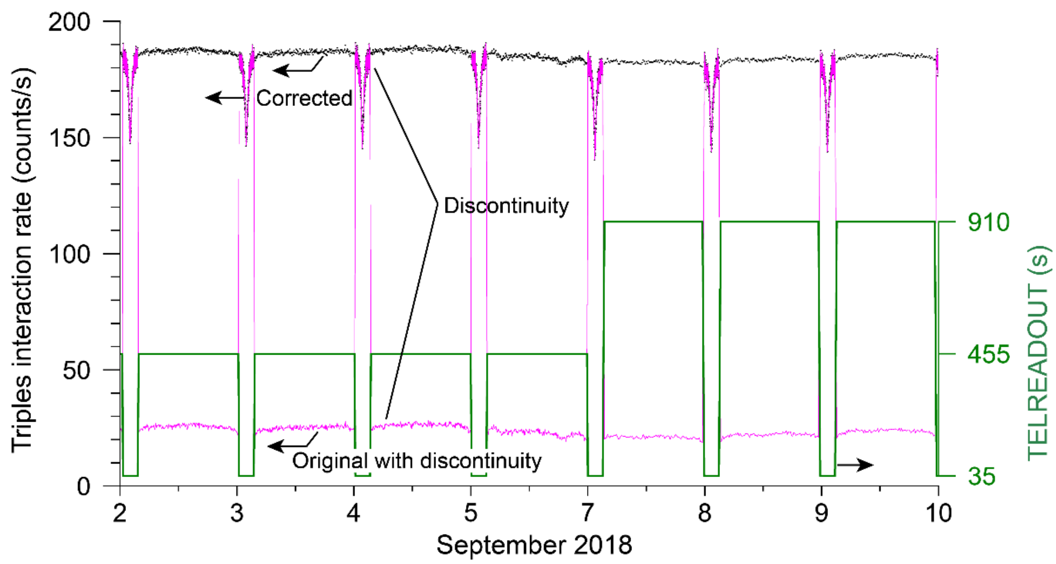

Figure 6. Time series of triples rates during the last mission phase at Ceres (C2E). The magenta trace shows triples rates from the ephemeris, pointing, and geometry file (GRD-L1B-150313-181026_190117-EPG.TAB). Discontinuities occur because the triples scaler rolls over for long accumulation times (TELREADOUT = 455- and 910 seconds, green trace). The new data file GRD_LIVETIME_TABLE.TAB properly accounts for roll over of the triples scaler, removing the discontinuity (black trace). Note that the dips that occur in both the magenta and black trace while TELREADOUT is set to 35 seconds result from the spacecraft passing through periapsis. Near periapsis, Ceres shields galactic cosmic rays resulting in a reduction in the triples rate. This effect was also observed around Mars Closest Approach (e.g. Fig. 2 and [16]).

A detailed discussion of how scaler roll over corrections for GRaND are made is found in [17]. GRaND does not have roll over counters. Instead, the number of times a scaler (16-bit counter) rolls over must be determined for each science accumulation from the time-series housekeeping telemetry, which is configured to subsample the accumulation interval. For example, when TELREADOUT = 210 seconds, we set TELSOH to 35 seconds, resulting in seven scaler samples (six from the housekeeping telemetry and the seventh from the science telemetry). This process is robust during quiet Sun conditions which occur for most science data records. The corrections may fail when particle fluxes are elevated during SEPs. As such, we have less confidence in the corrected counts reported in GRD_LIVETIME_TABLE during SEPs than for other observing conditions. During intense SEPs, abrupt changes in counts from the science telemetry indicate a scaler has rolled over. This information can be used in the reconstruction of particle fluxes; however, the live times presented in the new table are based entirely on information from the state-of-health telemetry.

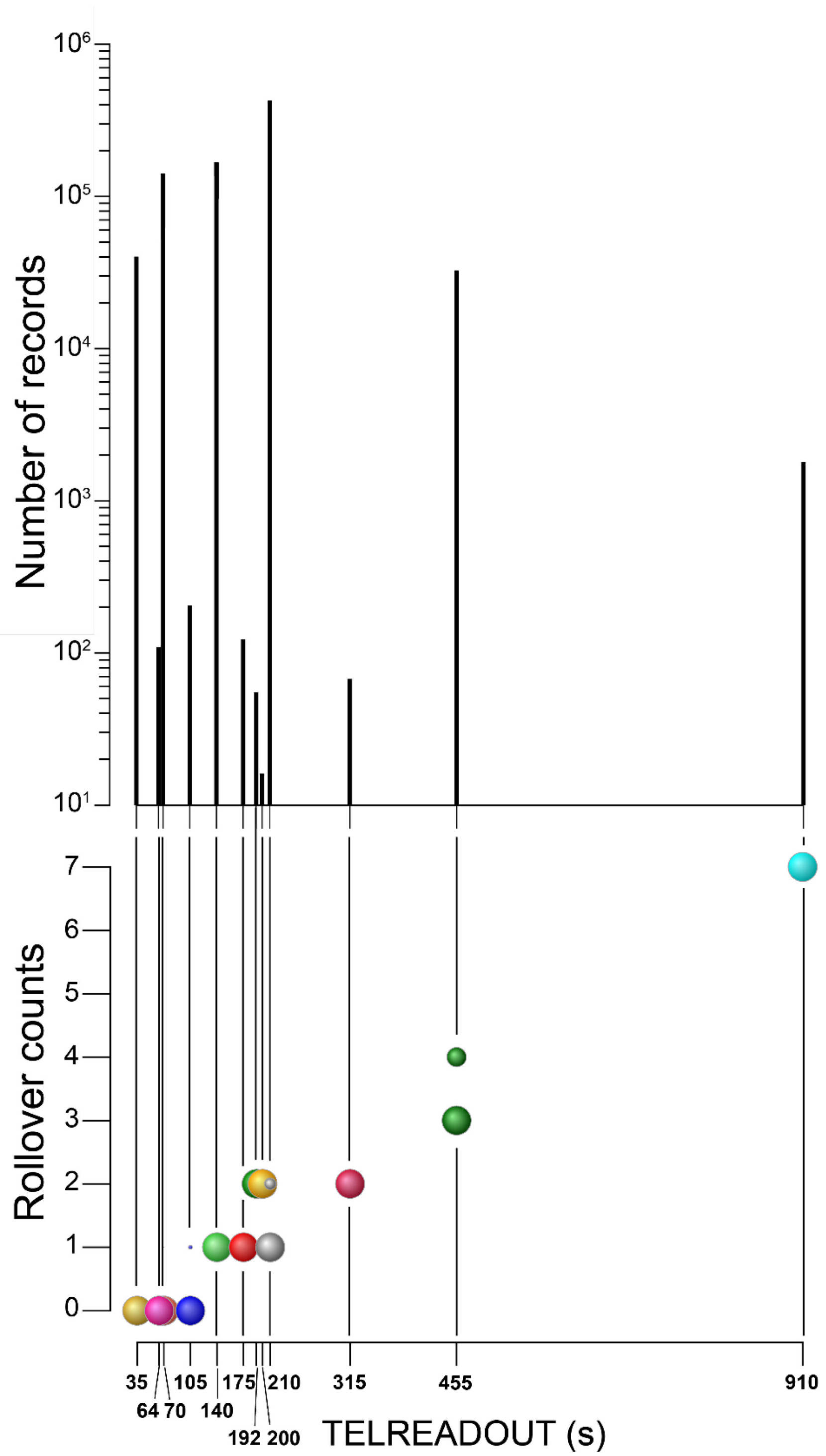

For quiet-Sun conditions, the dependence of the number of times the dead time scaler rolled over on the length of the science accumulation interval (TELREADOUT) is shown in Fig. 7. The number of roll overs, which was determined from the housekeeping telemetry, varies roughly linearly with TELREADOUT; however, for some TELREADOUT settings, the number of roll overs can take on more than one value. For example, the most frequent TELREADOUT setting during the mission was 210 seconds. With this setting, the roll over counts was most often 1 and less frequently 2. A similar bifurcation of roll over counts occurs for TELREADOUT is 455 seconds. The new live-time table fully accounts for these effects, allowing the user to make robust live time corrections for all records in the archive acquired under quiet Sun conditions.

Figure 7. Rollover counts for the dead time scaler as a function of the length of the science accumulation interval, TELREADOUT (lower panel). The number of records for which each setting occurred is shown in the top panel.

WHO CAN I CONTACT TO GET HELP?

Please address questions or concerns about the archive to Tom Prettyman (for questions about the instrument and data) and Carol Neese (for PDS archive questions). Or contact the PDS Operator at pds_operator@jpl.nasa.gov.

Thomas H. Prettyman, GRaND lead Planetary Science Institute prettyman@psi.edu 6509 Caballero Pkwy NW Los Ranchos de Albuquerque, New Mexico 87107	Carol Neese, PDS Small Bodies Node Planetary Science Institute neese@psi.edu 1700 E. Ft. Lowell, Ste. 106 Tucson, AZ 8571

ACKNOWLEDGEMENTS

Contributions to the GRaND investigation through development and flight are acknowledged by [16]. During the mission, data archiving was carried out by the GRaND team at PSI in collaboration with the UCLA Dawn Science Center (DSC). Steven Joy, Joseph Mafi, and Xinping Liu – all from the DSC – assisted in the development of the PDS3 archive, from retrieval of the telemetry data to delivery of the final data products to the PDS. We acknowledge members of the science community who critically evaluated the data prior to its release to the public. They include Larry Evans of GSFC (Vesta), Brad Jolliff of Washington University (Vesta), David Lawrence of JHU-APL (Mars/Cruise), Larry Nittler of Carnegie Mellon University (Mars/Cruise, Ceres), Ed Rhodes of JHU-APL (Vesta), and Dave Vaniman of PSI (Vesta and Ceres). Richard Chen (JPL) provided critical support for standards validation. The PDS4 migration project was carried out by the authors with funding from the NASA PDS and the NASA Discovery Program. Scientific evaluation of the data was supported by the NASA Discovery Data Analysis Program (Grant #80NSSC20K1153) and the NASA Solar System Exploration Research Virtual Institute (SSERVI) program's Toolbox for Research and Exploration. We thank Eric Palmer (PSI/SBN PI) and Margaret Landis (UC/LASP) for their contributions to the design and development of the GRaND PDS4 archive. For the NucSpec dictionary, the SBN received input from the authors as well as other researchers interested in planetary nuclear spectroscopy, including Craig Hardgrove (ASU) and Richard Starr (Catholic University of America). Members of the PDS community, including Joni Johnson (Atmospheres), Ron Joyner (Engineering), Todd King (PPI), Anne Raugh (SBN), and Scott VanBommell (Geosciences) also provided constructive feedback. The latest dictionaries used in the archive build on this initial effort.

APPENDIX

The state table is presented in Tables A1-2 (GRD_STATE_TABLE.TAB found in the dawn-grand-ancillary directory). Tables A3-6 list the observing conditions included in the labels for time-series data files.

Table A1. Instrument settings Part 1 – From GRD_STATE_TABLE.TAB. Each operational state is assigned an index (ID). The following information is tabulated for each state: The instrument mode (M), high voltage settings (HVPS1-6 with units of volts) and supply status (S=1 when enabled), status of low voltage supplies (A= PM5_LVPS; B= P12_LVPS; B= CZT_PM5_LVPS, enabled=1), the status of each of the 16 CZT sensors (CZT_enables, 1=disabled), the total number of gamma events allowed per science data record (NGAM), the number of CZT events (NCZT), and the number of neutron events (NEMN).

ID	M	HVPS1	S	HVPS2	S	HVPS3	S	HVPS4	S	HVPS5	S	HVPS6	S	A	B	C	CZT_ENABLES	NGAM	NCZT	NEMN
1	1	1058.82	1	1000.00	1	1029.41	1	1058.82	1	735.29	1	1000.00	1	1	1	1	0010000000000010	3876	3875	2800
2	1	1058.82	1	1000.00	1	1029.41	1	1058.82	1	735.29	1	1000.00	1	1	1	1	0010000000000010	3876	3875	2800
3	1	1058.82	1	1000.00	1	1029.41	1	1058.82	1	735.29	1	1000.00	1	1	1	1	0010000000000010	3876	3376	2800
4	1	1058.82	1	1000.00	1	1029.41	1	1088.24	1	735.29	1	1000.00	1	1	1	1	0010000000000010	3876	3376	2800
5	1	1058.82	1	1000.00	1	1029.41	1	1058.82	1	735.29	1	1000.00	1	1	1	1	0010000000000010	3876	3376	2800
6	1	1058.82	1	1000.00	1	1029.41	1	1058.82	1	735.29	1	1000.00	1	1	1	1	0010000000000010	3876	3376	2800
7	1	1058.82	1	1000.00	1	1029.41	1	1058.82	1	735.29	1	1000.00	1	1	1	1	0010000000000010	3876	3376	2800
8	1	1058.82	1	1000.00	1	1029.41	1	1088.24	1	735.29	1	1000.00	1	1	1	1	0010000000000010	3876	3376	2800
9	1	1058.82	1	1000.00	1	1029.41	1	1117.65	1	735.29	1	1000.00	1	1	1	1	0010000000000010	3876	3376	2800
10	1	1058.82	1	1000.00	1	1029.41	1	1058.82	1	735.29	1	1000.00	1	1	1	1	0010000000000010	3876	3376	2800
11	1	1058.82	1	1000.00	1	1029.41	1	1058.82	1	735.29	1	1000.00	1	1	1	1	0010001000000010	3876	3376	2800
12	1	1058.82	1	1000.00	1	1029.41	1	588.24	1	735.29	1	0.00	0	1	1	0	0010001000000010	3876	3376	2800
13	1	1058.82	1	1000.00	1	1029.41	1	1058.82	1	735.29	1	0.00	0	1	1	0	0010001000000010	3876	3376	2800
14	1	1058.82	1	1000.00	1	1029.41	1	1058.82	1	735.29	1	294.12	1	1	1	1	0010001000000010	3876	3376	2800
15	1	1088.24	1	1000.00	1	1029.41	1	1058.82	1	735.29	1	1000.00	1	1	1	1	0010001000000010	3876	3376	2800
16	1	1058.82	1	1000.00	1	1029.41	1	1058.82	1	735.29	1	1000.00	1	1	1	1	0010001000000010	3876	3376	2800
17	1	1058.82	1	1000.00	1	1029.41	1	1058.82	1	700.00	1	1000.00	1	1	1	1	0010001000000010	3876	3376	2800
18	1	1058.82	1	1000.00	1	1029.41	1	1058.82	1	711.76	1	1000.00	1	1	1	1	0010001000000010	3876	3376	2800
19	1	1058.82	1	1000.00	1	1029.41	1	1058.82	1	723.53	1	1000.00	1	1	1	1	0010001000000010	3876	3376	2800
20	1	1058.82	1	1000.00	1	1029.41	1	1058.82	1	747.06	1	1000.00	1	1	1	1	0010001000000010	3876	3376	2800
21	1	1058.82	1	1000.00	1	1029.41	1	1058.82	1	752.94	1	1000.00	1	1	1	1	0010001000000010	3876	3376	2800
22	1	1088.24	1	1017.65	1	1047.06	1	1070.59	1	723.53	1	1000.00	1	1	1	1	0010001000000010	3876	3376	2800
23	1	1088.24	1	1017.65	1	1047.06	1	1070.59	1	711.76	1	1000.00	1	1	1	1	0010001000000010	3876	3376	2800
24	1	1088.24	1	1017.65	1	1047.06	1	1070.59	1	700.00	1	1000.00	1	1	1	1	0010001000000010	3876	3376	2800
25	1	1088.24	1	1017.65	1	1047.06	1	1070.59	1	747.06	1	1000.00	1	1	1	1	0010001000000010	3876	3376	2800

Table A2. Instrument settings Part 2 – From GRD_STATE_TABLE.TAB. For each state: The upper and lower bounds (in channels) for the coincidence windows and regions of interest for the BGO and plastic scintillators.

	BGO				BLP_MY				BLP_PY				BLP_MZ				BLP_PZ			
	CW		ROI		CW		ROI		CW		ROI		CW		ROI		CW		ROI	
ID	L	H	L	H	L	H	L	H	L	H	L	H	L	H	L	H	L	H	L	H
1	35	52	25	88	15	44	1	64	17	43	1	64	15	30	1	64	10	40	1	64
2	35	51	15	78	12	46	1	64	16	50	1	64	10	40	1	64	10	40	1	64
3	27	52	15	78	5	50	1	64	5	50	1	64	5	50	1	64	5	50	1	64
4	27	52	15	78	5	50	1	64	5	50	1	64	5	50	1	64	5	50	1	64
5	1	64	1	64	5	50	1	64	5	50	1	64	5	50	1	64	5	50	1	64
6	9	25	1	64	12	44	1	64	15	40	1	64	12	40	1	64	5	50	1	64
7	12	22	1	64	12	44	1	64	15	40	1	64	12	40	1	64	5	50	1	64
8	12	22	1	64	12	44	1	64	15	40	1	64	1	64	1	64	5	50	1	64
9	12	22	1	64	12	44	1	64	15	40	1	64	1	64	1	64	5	50	1	64
10	1	64	1	64	1	64	1	64	1	64	1	64	1	64	1	64	1	64	1	64
11	1	64	1	64	1	64	1	64	1	64	1	64	1	64	1	64	1	64	1	64
12	1	64	1	64	1	64	1	64	1	64	1	64	1	64	1	64	1	64	1	64
13	1	64	1	64	1	64	1	64	1	64	1	64	1	64	1	64	1	64	1	64
14	1	64	1	64	1	64	1	64	1	64	1	64	1	64	1	64	1	64	1	64
15	7	25	1	64	1	64	1	64	1	64	1	64	1	64	1	64	1	64	1	64
16	7	25	1	64	1	64	1	64	1	64	1	64	1	64	1	64	1	64	1	64
17	1	64	1	64	1	64	1	64	1	64	1	64	1	64	1	64	1	64	1	64
18	1	64	1	64	1	64	1	64	1	64	1	64	1	64	1	64	1	64	1	64
19	1	64	1	64	1	64	1	64	1	64	1	64	1	64	1	64	1	64	1	64
20	1	64	1	64	1	64	1	64	1	64	1	64	1	64	1	64	1	64	1	64
21	1	64	1	64	1	64	1	64	1	64	1	64	1	64	1	64	1	64	1	64
22	1	64	1	64	1	64	1	64	1	64	1	64	1	64	1	64	1	64	1	64
23	1	64	1	64	1	64	1	64	1	64	1	64	1	64	1	64	1	64	1	64
24	1	64	1	64	1	64	1	64	1	64	1	64	1	64	1	64	1	64	1	64
25	1	64	1	64	1	64	1	64	1	64	1	64	1	64	1	64	1	64	1	64

Table A3. Observing conditions: Solar energetic particles (SEP).

UTC start	UTC stop	SCLK start	SCLK stop	ID	Description
2011-06-03T23:59:04	2011-06-22T23:58:34	360417716	362059286	VSA	SEP
2011-08-04T12:02:13	2011-08-12T23:58:14	365731505	366465665	VSA	SEP
2011-11-04T00:02:05	2011-11-08T05:56:35	373637097	374003967	VTL	SEP
2012-01-25T06:22:06	2012-02-08T23:58:40	380744628	382017622	VSL	SEP
2012-03-06T17:59:33	2012-04-02T17:58:43	384328875	386661625	VSL	SEP
2012-07-23T00:01:04	2012-08-02T12:01:03	396273837	397181037	VH2	SEP

UTC start	UTC stop	SCLK start	SCLK stop	ID	Description
2015-03-24T18:00:33	2015-03-31T11:56:33	480492205	481075165	CSA	SEP
2015-04-21T12:00:03	2015-04-29T23:57:30	482889775	483624022	CSA	SEP
2015-05-02T00:01:30	2015-05-08T11:57:00	483797062	484358392	CSR	SEP
2015-06-18T00:01:24	2015-06-27T23:56:54	487857856	488721586	CSS	SEP + energetic electron bursts
2015-10-28T23:59:04	2015-11-06T23:56:04	499348918	500126338	CTL	SEP
2017-07-23T11:59:41	2017-08-10T23:58:11	554083355	555681665	CX2	SEP
2017-09-10T18:00:11	2017-09-28T23:58:11	558338585	559915265	CX2	SEP

Table A4. Observing conditions: Solar flare (SF) X-rays. Solar flare X-rays were identified in the GRaND data by correlation with data from the NOAA Geostationary Operational Environmental Satellite (GOES).

UTC start	UTC stop	SCLK start	SCLK stop	ID	Description
2011-08-04T03:52:13	2011-08-04T04:16:43	365702105	365703575	VSA	Solar flare - M9.3
2011-09-06T01:42:13	2011-09-06T02:06:43	368545505	368546975	VTH	Solar flare - M5.3
2011-09-06T22:17:43	2011-09-06T22:42:13	368619635	368621105	VTH	Solar flare - X2.1
2011-09-07T22:33:43	2011-09-07T22:58:13	368706995	368708465	VTH	Solar flare - X1.8
2011-09-08T15:42:43	2011-09-08T16:07:13	368768735	368770205	VTH	Solar flare - M6.7
2011-11-02T21:57:35	2011-11-02T22:18:35	373543227	373544487	VSH	Solar flare - M4.3
2011-11-03T20:21:35	2011-11-03T20:46:05	373623867	373625337	VTL	Solar flare - X1.9
2012-06-02T04:33:35	2012-06-02T04:58:05	391883787	391885257	VT2	Solar flare - C1.5
2012-07-06T23:08:04	2012-07-06T23:29:04	394888257	394889517	VH2	Solar flare - X1.1
2015-04-21T15:44:03	2015-04-21T16:08:33	482903215	482904685	CSA	Solar flare - M4.0
2015-04-21T17:08:03	2015-04-21T17:25:33	482908255	482909305	CSA	Solar flare - M2.1
2015-11-09T13:11:04	2015-11-09T13:35:34	500346838	500348308	CTL	Solar flare - M3.9
2017-09-06T09:07:11	2017-09-06T09:35:11	557961005	557962685	CX2	Solar flare - X2
2017-09-06T11:58:41	2017-09-06T12:23:11	557971295	557972765	CX2	Solar flare - X9
2017-09-07T10:15:41	2017-09-07T10:40:11	558051515	558052985	CX2	Solar flare - M7
2017-09-07T14:34:41	2017-09-07T14:59:11	558067055	558068525	CX2	Solar flare - X1
2017-09-10T15:57:41	2017-09-10T16:22:11	558331235	558332705	CX2	Solar flare - X8

Table A5. Observing conditions: Gamma-ray bursts (GRBs). GRBs were identified in the GRaND science telemetry by correlation with the Fermi Gamma-ray telescope [27]. The GRB name and Fermi trigger time are included in the description of each burst.

UTC start	UTC stop	SCLK start	SCLK stop	ID	Description
2011-09-20T13:01:13	2011-09-20T13:15:13	369795845	369796685	VTH	GRB110920546 Fermi trigger: 2011-09-20 13:05:43.812
2012-02-04T00:59:50	2012-02-04T01:04:30	381589292	381589572	VSL	GRB120204054 Fermi trigger: 2012-02-04 01:17:07.832
2012-04-20T20:29:55	2012-04-20T20:34:35	388225897	388226177	VSL	GRB120420858 Fermi trigger: 2012-04-20 20:35:13.070
2012-05-26T06:50:05	2012-05-26T07:04:05	391287177	391288017	VT2	GRB120526303 Fermi trigger: 2012-05-26 07:16:40.770
2012-06-24T22:23:05	2012-06-24T22:37:05	393848757	393849597	VH2	GRB120624933 Fermi trigger: 2012-06-24 22:23:54.934
2012-07-11T02:39:04	2012-07-11T02:53:04	395246517	395247357	VH2	GRB120711115 Fermi trigger: 2012-07-11 02:44:53.294
2015-03-30T19:43:33	2015-03-30T19:57:33	481016785	481017625	CSA	GRB150330828 Fermi trigger: 2015-03-30 19:52:21.265
2015-06-27T04:20:54	2015-06-27T04:34:54	488651026	488651866	CSS	GRB150627183 Fermi trigger: 2015-06-27 04:23:23.681

UTC start	UTC stop	SCLK start	SCLK stop	ID	Description
2016-05-09T08:51:57	2016-05-09T09:01:17	516056057	516056617	CSL	GRB160509374 Fermi trigger: 2016-05-09 08:58:46.219
2016-08-21T20:40:44	2016-08-21T20:50:04	525084183	525084743	CXL	GRB160821857 Fermi trigger: 2016-08-21 20:34:30.039
2017-02-14T15:46:12	2017-02-14T16:00:12	540359347	540360187	CXG	GRB170214649 Fermi trigger: 2017-02-14 15:34:26.924
2017-04-09T02:24:13	2017-04-09T02:38:13	544976827	544977667	CTO	GRB170409112 Fermi trigger: 2017-04-09 02:42:00.490
2017-09-06T00:43:11	2017-09-06T00:57:11	557930765	557931605	CX2	GRB170906030 Fermi trigger: 2017-09-06 00:43:08.152
2017-10-10T18:46:11	2017-10-10T19:00:11	560933345	560934185	CX2	GRB171010792 Fermi trigger: 2017-10-10 19:00:50.576
2011-06-18T08:44:04	2011-06-18T08:51:04	361658816	361659236	VSA	GRB110618366 Fermi trigger: 2011-06-18 08:47:36.383
2012-03-28T06:47:13	2012-03-28T06:49:33	386189335	386189475	VSL	GRB120328268 Fermi trigger: 2012-03-28 06:26:20.953
2015-03-15T09:50:03	2015-03-15T09:57:03	479685175	479685595	CSA	GRB150314205 Fermi trigger: 2015-03-14 04:54:50.854
2015-05-10T03:09:00	2015-05-10T03:16:00	484499512	484499932	CTS	GRB150510139 Fermi trigger: 2015-05-10 03:19:53.738
2015-08-21T09:24:58	2015-08-21T09:40:08	493421394	493422304	CSH	GRB150821406 Fermi trigger: 2015-08-21 09:44:20.332
2016-04-21T03:10:17	2016-04-21T03:14:57	514480357	514480637	CSL	GRB160421137 Fermi trigger: 2016-04-21 03:17:33.153
2016-06-25T22:36:17	2016-06-25T22:40:57	520166317	520166597	CXL	GRB160625945 Fermi trigger: 2016-06-25 22:40:16.275
2016-07-20T18:15:58	2016-07-20T18:20:38	522310697	522310977	CXL	GRB160720767 Fermi trigger: 2016-07-20 18:23:56.999
2016-09-05T11:23:41	2016-09-05T11:30:41	526346794	526347214	CTJ	GRB160905471 Fermi trigger: 2016-09-05 11:18:55.912
2016-12-18T08:10:41	2016-12-18T08:17:41	535320814	535321234	CXG	GRB161218356 Fermi trigger: 2016-12-18 08:32:40.647
2017-02-10T02:58:42	2017-02-10T03:05:42	539967697	539968117	CXG	GRB170210116 Fermi trigger: 2017-02-10 02:47:36.576
2017-04-05T19:04:13	2017-04-05T19:11:13	544691227	544691647	CTO	GRB170405777 Fermi trigger: 2017-04-05 18:39:22.886
2017-05-27T11:44:37	2017-05-27T11:51:37	549157651	549158071	CXO	GRB170527480 Fermi trigger: 2017-05-27 11:31:02.374
2017-06-07T23:08:07	2017-06-07T23:15:07	550149061	550149481	CXO	GRB170607946 Fermi trigger: 2017-06-07 23:17:59.567
2017-08-08T22:05:41	2017-08-08T22:12:41	555502115	555502535	CX2	GRB170808936 Fermi trigger: 2017-08-08 22:27:43.098
2017-11-19T23:39:41	2017-11-19T23:46:41	564406955	564407375	CX2	GRB171119992 Fermi trigger: 2017-11-19 23:48:27.172
2017-12-10T11:56:11	2017-12-10T12:03:11	566179145	566179565	CX2	GRB171210493 Fermi trigger: 2017-12-10 11:49:15.261
2017-12-27T00:08:11	2017-12-27T00:15:11	567605465	567605885	CX2	GRB171227000 Fermi trigger: 2017-12-27 00:00:13.402
2018-01-13T09:58:41	2018-01-13T10:05:41	569109695	569110115	CX2	GRB180113418 Fermi trigger: 2018-01-13 10:02:05.407
2018-01-20T04:40:11	2018-01-20T04:47:11	569695385	569695805	CX2	GRB180120207 Fermi trigger: 2018-01-20 04:58:13.000
2018-02-10T12:25:40	2018-02-10T12:32:40	571537715	571538135	CX2	GRB180210517 Fermi trigger: 2018-02-10 12:24:38.548
2018-03-05T09:17:10	2018-03-05T09:24:10	573513605	573514025	CX2	GRB180305393 Fermi trigger: 2018-03-05 09:26:08.661
2018-07-20T14:37:39	2018-07-20T14:52:49	585369755	585370665	C2E	GRB180720598 Fermi trigger: 2018-07-20 14:21:39.654

Table A6. Data glitch (DG). The descriptions include the following notation: GSD detect - Detection of a blip or dip using a Gaussian second difference filter; /\ - A blip (rapid rise followed by return to baseline); \/ - A dip (rapid drop followed by return to the baseline); \/\ - Detection of a sawtooth consisting of a dip below the baseline (first record) followed by a rise above the baseline (second record) and immediate return to the baseline. Blips may result from unidentified GRBs or solar flare X-rays. Dips and sawtooths are likely instrument glitches.

UTC start	UTC stop	SCLK start	SCLK stop	ID	Description
2011-09-20T23:59:13	2011-10-12T23:56:35	369835325	371735967	VTH	BGO anomaly
2011-06-09T02:04:34	2011-06-09T02:25:34	360857246	360858506	VSA	PHOS_PZ - Data glitch \/\
2011-06-22T17:47:34	2011-06-22T18:05:04	362037026	362038076	VSA	PHOS_PZ - Data glitch \/\
2011-08-09T08:07:14	2011-08-09T08:21:14	366149405	366150245	VSA	PHOS_PZ overload - Blip /\
2012-03-30T04:58:03	2012-03-30T05:03:53	386355585	386355935	VSL	PHOS_PZ - Data glitch \/\
2015-03-29T05:06:33	2015-03-29T05:24:03	480877765	480878815	CSA	PHOS_PZ - Blip /\
2015-03-30T19:40:03	2015-03-30T19:57:33	481016575	481017625	CSA	PHOS_PZ - Blip /\
2015-05-03T20:25:00	2015-05-03T20:39:00	483956872	483957712	CSR	PHOS_PZ overload - Blip /\
2015-05-07T00:22:00	2015-05-07T00:36:00	484230292	484231132	CSR	PHOS_PZ - Blip /\
2009-01-24T06:02:48	2009-01-24T06:07:49	286049052	286049353	MGA	GSD detect
2009-03-14T18:38:14	2009-03-14T19:02:44	290328066	290329536	MGA	GSD detect
2009-03-21T14:22:44	2009-03-21T14:50:44	290917536	290919216	MGA	GSD detect

UTC start	UTC stop	SCLK start	SCLK stop	ID	Description
2011-05-04T10:23:04	2011-05-04T10:51:04	357776756	357778436	VSA	GSD detect
2011-05-09T17:54:04	2011-05-09T18:18:34	358235816	358237286	VSA	GSD detect
2011-05-18T02:09:34	2011-05-18T02:30:34	358956746	358958006	VSA	GSD detect
2011-05-22T15:21:34	2011-05-22T15:46:04	359349866	359351336	VSA	GSD detect
2011-06-01T12:01:04	2011-06-01T12:25:34	360201836	360203306	VSA	GSD detect
2011-07-10T16:13:13	2011-07-10T16:37:43	363586565	363588035	VSA	GSD detect
2011-08-02T10:16:43	2011-08-02T10:44:43	365552375	365554055	VSA	GSD detect
2011-08-29T17:42:43	2011-08-29T18:07:13	367911935	367913405	VSS	GSD detect
2011-09-06T07:46:13	2011-09-06T08:10:43	368567345	368568815	VTH	GSD detect
2011-09-19T05:13:43	2011-09-19T05:41:43	369681395	369683075	VTH	GSD detect
2011-10-29T01:59:35	2011-10-29T02:27:35	373125747	373127427	VSH	GSD detect
2011-12-08T10:48:12	2011-12-08T10:56:22	376613394	376613884	VTL	GSD detect
2011-12-09T04:59:02	2011-12-09T05:07:12	376678844	376679334	VTL	GSD detect
2011-12-16T19:02:32	2011-12-16T19:10:42	377334254	377334744	VSL	GSD detect
2011-12-27T09:54:02	2011-12-27T10:02:12	378251744	378252234	VSL	GSD detect
2012-01-09T07:23:52	2012-01-09T07:30:52	379365934	379366354	VSL	GSD detect
2012-02-17T03:26:00	2012-02-17T03:33:00	382721262	382721682	VSL	GSD detect
2012-03-01T09:11:33	2012-03-01T09:20:53	383865195	383865755	VSL	GSD detect
2012-04-22T17:17:55	2012-04-22T17:24:55	388387177	388387597	VSL	GSD detect
2012-05-02T13:57:25	2012-05-02T14:03:15	389239147	389239497	VT2	GSD detect
2012-05-20T00:27:05	2012-05-20T00:51:35	390745797	390747267	VT2	GSD detect
2012-06-03T10:25:35	2012-06-03T10:50:05	391991307	391992777	VT2	GSD detect
2012-07-02T06:12:04	2012-07-02T06:36:34	394481697	394483167	VH2	GSD detect
2012-12-12T22:25:33	2012-12-12T22:50:03	408623306	408624776	VCC	GSD detect
2015-07-29T18:52:11	2015-07-29T19:16:41	491468104	491469574	CTH	GSD detect
2015-08-01T01:59:41	2015-08-01T02:20:41	491666554	491667814	CTH	GSD detect
2015-08-06T07:03:41	2015-08-06T07:24:41	492116794	492118054	CTH	GSD detect
2015-08-06T08:55:41	2015-08-06T09:20:11	492123514	492124984	CTH	GSD detect
2015-08-16T23:47:10	2015-08-17T00:11:40	493041004	493042474	CTH	GSD detect
2015-09-01T03:37:43	2015-09-01T04:30:48	494350959	494354144	CSH	GSD detect
2015-10-11T08:28:53	2015-10-11T09:21:58	497824429	497827614	CSH	GSD detect
2015-10-21T23:24:27	2015-10-22T00:17:32	498742164	498745349	CSH	GSD detect
2015-11-10T16:53:34	2015-11-10T17:18:04	500446588	500448058	CTL	GSD detect
2016-01-27T19:56:18	2016-01-27T20:12:38	507196717	507197697	CSL	GSD detect
2016-03-18T15:38:58	2016-03-18T15:57:38	511587677	511588797	CSL	GSD detect
2016-05-11T12:09:37	2016-05-11T12:28:17	516240717	516241837	CSL	GSD detect
2016-06-22T23:40:17	2016-06-22T23:54:17	519910957	519911797	CXL	GSD detect
2016-07-11T22:42:37	2016-07-11T22:58:57	521549097	521550077	CXL	GSD detect
2016-09-09T02:39:41	2016-09-09T03:04:11	526660954	526662424	CTJ	GSD detect
2016-09-09T20:51:41	2016-09-09T21:16:11	526726474	526727944	CTJ	GSD detect
2016-09-27T07:34:41	2016-09-27T07:59:11	528233854	528235324	CTJ	GSD detect
2016-11-14T02:26:41	2016-11-14T02:51:11	532362574	532364044	CTG	GSD detect
2016-11-26T23:54:11	2016-11-27T00:18:41	533476624	533478094	CTG	GSD detect
2016-11-27T18:06:11	2016-11-27T18:30:41	533542144	533543614	CTG	GSD detect
2017-01-01T15:31:40	2017-01-01T15:56:10	536556874	536558344	CXG	GSD detect
2017-01-07T17:11:10	2017-01-07T17:32:10	537081244	537082504	CXG	GSD detect
2017-01-09T05:35:10	2017-01-09T05:59:40	537212284	537213754	CXG	GSD detect
2017-01-12T06:23:11	2017-01-12T06:47:41	537474365	537475835	CXG	GSD detect
2017-03-25T12:31:12	2017-03-25T12:55:42	543717247	543718717	CTO	GSD detect
2017-05-25T09:45:07	2017-05-25T10:09:37	548977681	548979151	CXO	GSD detect

UTC start	UTC stop	SCLK start	SCLK stop	ID	Description
2017-06-14T21:18:41	2017-06-14T21:39:41	550747295	550748555	CXO	GSD detect
2017-07-19T00:29:11	2017-07-19T00:53:41	553696325	553697795	CX2	GSD detect
2017-07-19T18:41:11	2017-07-19T19:05:41	553761845	553763315	CX2	GSD detect
2017-07-22T19:25:41	2017-07-22T19:50:11	554023715	554025185	CX2	GSD detect
2017-08-19T02:51:41	2017-08-19T03:16:11	556383275	556384745	CX2	GSD detect
2017-10-05T21:45:11	2017-10-05T22:09:41	560512085	560513555	CX2	GSD detect
2017-10-19T13:24:41	2017-10-19T13:52:41	561691655	561693335	CX2	GSD detect
2017-11-07T12:31:41	2017-11-07T12:56:11	563330075	563331545	CX2	GSD detect
2017-11-17T09:07:41	2017-11-17T09:35:41	564181835	564183515	CX2	GSD detect
2017-11-23T10:50:41	2017-11-23T11:15:11	564706415	564707885	CX2	GSD detect
2018-01-19T08:11:41	2018-01-19T08:32:41	569621675	569622935	CX2	GSD detect
2018-02-11T02:18:40	2018-02-11T02:43:10	571587695	571589165	CX2	GSD detect
2018-04-24T03:43:11	2018-04-24T04:07:41	577813565	577815035	CTI	GSD detect
2018-05-09T07:50:11	2018-05-09T08:11:11	579124385	579125645	CTI	GSD detect
2018-05-18T10:14:46	2018-05-18T10:39:16	579910660	579912130	C2I	GSD detect
2018-06-20T18:54:19	2018-06-20T19:54:59	582793155	582796795	C2E	GSD detect
2018-06-23T01:41:19	2018-06-23T02:31:33	582990375	582993179	C2E	GSD detect
2018-06-26T02:28:03	2018-06-26T03:21:08	583252379	583255564	C2E	GSD detect
2018-07-08T05:42:30	2018-07-08T06:43:10	584300846	584304486	C2E	GSD detect
2018-08-15T22:00:10	2018-08-15T23:00:50	587642706	587646346	C2E	GSD detect
2018-10-17T20:40:52	2018-10-17T21:03:34	593081148	593082300	C2E	GSD detect
2009-03-03T09:38:14	2009-03-03T09:48:44	289345266	289345896	MGA	Manual removal of data glitch \/\
2015-06-03T22:47:54	2015-06-03T22:58:24	486643846	486644476	CSS	Manual removal of data glitch \/\
2015-08-14T17:14:41	2015-08-14T17:25:11	492844654	492845284	CTH	Manual removal of data glitch \/\
2016-11-09T13:14:41	2016-11-09T13:32:11	531969454	531970504	CTG	Manual removal of blip /\
2017-11-25T09:34:11	2017-11-25T09:55:11	564874625	564875885	CX2	Manual removal of blip /\
2018-06-15T03:45:03	2018-06-15T03:58:58	582306599	582307224	C2E	Manual removal of blip /\
2018-09-02T09:05:24	2018-09-02T09:28:09	589151420	589152785	C2E	Manual removal of blip /\
2011-06-09T02:12:07	2011-06-09T02:18:34	360857699	360858086	VSA	Manual removal of down-up glitch \/\
2011-06-22T17:58:04	2011-06-22T17:58:04	362037656	362037656	VSA	Manual removal of blip /\
2011-08-09T08:14:14	2011-08-09T08:14:14	366149825	366149825	VSA	Manual removal of blip \/ (X6.9 solar flare?)
2012-02-29T11:03:53	2012-02-29T11:03:53	383785535	383785535	VSL	Manual removal of BGO and PZ anomaly (truncated spectrum)
2012-02-29T18:40:03	2012-02-29T18:40:03	383812905	383812905	VSL	Manual removal of BGO anomaly (truncated spectrum)
2012-02-29T19:18:33	2012-02-29T19:18:33	383815215	383815215	VSL	Manual removal of BGO anomaly (truncated spectrum)
2012-02-29T21:40:53	2012-02-29T21:40:53	383823755	383823755	VSL	Manual removal of BGO anomaly (truncated spectrum)
2012-02-29T22:07:43	2012-02-29T22:07:43	383825365	383825365	VSL	Manual removal of BGO anomaly (truncated spectrum)
2012-02-29T22:12:23	2012-02-29T22:12:23	383825645	383825645	VSL	Manual removal of BGO anomaly (truncated spectrum)
2012-02-29T22:24:03	2012-02-29T22:24:03	383826345	383826345	VSL	Manual removal of BGO anomaly (truncated spectrum)
2012-02-29T22:34:33	2012-02-29T22:34:33	383826975	383826975	VSL	Manual removal of BGO anomaly (truncated spectrum)
2012-02-29T22:40:23	2012-02-29T22:40:23	383827325	383827325	VSL	Manual removal of BGO anomaly (truncated spectrum)
2012-02-29T22:50:53	2012-02-29T22:50:53	383827955	383827955	VSL	Manual removal of BGO and PZ anomaly (truncated spectrum)
2012-02-29T23:29:23	2012-02-29T23:29:23	383830265	383830265	VSL	Manual removal of BGO anomaly (truncated spectrum)
2012-03-01T00:41:43	2012-03-01T00:41:43	383834605	383834605	VSL	Manual removal of BGO anomaly (truncated spectrum)
2012-03-01T00:49:53	2012-03-01T00:49:53	383835095	383835095	VSL	Manual removal of BGO anomaly (truncated spectrum)
2012-03-01T01:45:53	2012-03-01T01:45:53	383838455	383838455	VSL	Manual removal of BGO and PZ anomaly (truncated spectrum)
2012-03-01T01:49:23	2012-03-01T01:49:23	383838665	383838665	VSL	Manual removal of BGO anomaly (truncated spectrum)
2012-03-01T03:30:53	2012-03-01T03:30:53	383844755	383844755	VSL	Manual removal of BGO anomaly (truncated spectrum)
2012-03-01T03:51:53	2012-03-01T03:51:53	383846015	383846015	VSL	Manual removal of BGO and PZ anomaly (truncated spectrum)
2012-03-01T04:01:13	2012-03-01T04:01:13	383846575	383846575	VSL	Manual removal of BGO anomaly (truncated spectrum)
2012-03-01T04:33:53	2012-03-01T04:33:53	383848535	383848535	VSL	Manual removal of BGO and PZ anomaly (truncated spectrum)

UTC start	UTC stop	SCLK start	SCLK stop	ID	Description
2012-03-01T07:53:23	2012-03-01T07:53:23	383860505	383860505	VSL	Manual removal of BGO anomaly (truncated spectrum)
2012-03-01T19:29:53	2012-03-01T19:29:53	383902295	383902295	VSL	Manual removal of BGO anomaly (truncated spectrum)
2012-02-29T21:45:33	2012-02-29T21:45:33	383824035	383824035	VSL	Manual removal of PZ anomaly (truncated spectrum)
2012-02-29T23:01:23	2012-02-29T23:01:23	383828585	383828585	VSL	Manual removal of PZ anomaly (truncated spectrum)
2012-03-01T01:47:03	2012-03-01T01:47:03	383838525	383838525	VSL	Manual removal of PZ anomaly (truncated spectrum)
2012-03-01T05:07:43	2012-03-01T05:07:43	383850565	383850565	VSL	Manual removal of PZ anomaly (truncated spectrum)
2011-10-16T22:19:35	2011-10-16T22:40:35	372075747	372077007	VSH	Manual removal of blip /\
2012-02-25T04:40:13	2012-02-25T04:47:13	383416915	383417335	VSL	Manual removal of blip \/
2012-04-18T14:41:45	2012-04-18T14:48:45	388032207	388032627	VSL	Manual removal of blip /\
2015-03-14T05:04:33	2015-03-14T05:25:33	479581645	479582905	CSA	Manual removal of blip /\
2015-03-16T20:50:03	2015-03-16T21:14:33	479811175	479812645	CSA	Manual removal of blip /\
2015-03-17T14:13:03	2015-03-17T14:37:33	479873755	479875225	CSA	Manual removal of blip /\
2015-04-03T21:26:03	2015-04-03T21:47:03	481368535	481369795	CSA	Manual removal of blip /\
2015-04-11T19:15:03	2015-04-11T19:36:03	482051875	482053135	CSA	Manual removal of blip \/
2015-04-12T10:56:33	2015-04-12T11:17:33	482108365	482109625	CSA	Manual removal of blip /\
2015-07-25T08:31:41	2015-07-25T08:52:41	491085274	491086534	CTH	Manual removal of blip /\
2015-08-16T11:04:11	2015-08-16T11:25:11	492995224	492996484	CTH	Manual removal of blip \/
2015-10-21T00:31:52	2015-10-21T01:24:57	498659809	498662994	CSH	Manual removal of blip /\
2015-10-25T04:17:04	2015-10-25T04:38:04	499018798	499020058	CTL	Manual removal of blip \/
2015-10-25T09:39:04	2015-10-25T09:56:34	499038118	499039168	CTL	Manual removal of blip \/
2015-10-26T18:57:34	2015-10-26T19:22:04	499158028	499159498	CTL	Manual removal of blip \/
2015-09-28T14:59:58	2015-09-28T15:53:03	496724694	496727879	CSH	Manual removal of blip /\
2016-01-31T08:19:38	2016-01-31T08:33:38	507500517	507501357	CSL	Manual removal of blip /\
2016-02-09T02:47:38	2016-02-09T03:01:38	508258197	508259037	CSL	Manual removal of blip /\
2016-03-10T16:16:38	2016-03-10T16:30:38	510898737	510899577	CSL	Manual removal of blip /\
2016-03-12T19:45:58	2016-03-12T19:57:38	511084097	511084797	CSL	Manual removal of blip /\
2016-06-23T04:45:57	2016-06-23T04:59:57	519929297	519930137	CXL	Manual removal of blip /\
2016-08-29T13:56:44	2016-08-29T14:10:44	525751143	525751983	CXL	Manual removal of blip /\
2017-02-28T19:12:42	2017-02-28T19:33:42	541581337	541582597	CTO	Manual removal of blip /\
2017-03-04T05:24:12	2017-03-04T05:45:12	541877227	541878487	CTO	Manual removal of blip /\
2017-04-10T01:33:43	2017-04-10T01:58:13	545060197	545061667	CTO	Manual removal of blip /\
2017-04-10T07:09:43	2017-04-10T07:30:43	545080357	545081617	CTO	Manual removal of blip /\
2017-04-10T22:19:43	2017-04-10T22:40:43	545134957	545136217	CTO	Manual removal of blip /\
2017-05-22T23:18:07	2017-05-22T23:39:07	548767261	548768521	CXO	Manual removal of blip /\
2017-06-01T08:31:37	2017-06-01T08:52:37	549578071	549579331	CXO	Manual removal of blip /\
2017-07-23T04:52:41	2017-07-23T05:13:41	554057735	554058995	CX2	Manual removal of blip /\
2017-10-11T00:36:11	2017-10-11T01:00:41	560954345	560955815	CX2	Manual removal of blip /\
2017-12-29T09:49:41	2017-12-29T10:14:11	567813155	567814625	CX2	Manual removal of blip /\
2018-01-03T00:57:11	2018-01-03T01:18:11	568213205	568214465	CX2	Manual removal of blip /\
2018-01-12T16:14:41	2018-01-12T16:35:41	569045855	569047115	CX2	Manual removal of blip /\
2018-01-30T01:09:10	2018-01-30T01:26:40	570546725	570547775	CX2	Manual removal of blip /\
2018-02-18T14:58:10	2018-02-18T15:15:40	572238065	572239115	CX2	Manual removal of blip /\
2018-02-23T05:58:40	2018-02-23T06:16:10	572637695	572638745	CX2	Manual removal of blip /\
2018-03-21T20:08:40	2018-03-21T20:26:10	574935095	574936145	CX2	Manual removal of blip /\
2018-04-04T21:18:41	2018-04-04T21:39:41	576148895	576150155	CX2	Manual removal of blip /\

REFERENCES

[1] Prettyman, T. H. *et al.* Elemental mapping by Dawn reveals exogenic H in Vesta's regolith. *Science* **338**, 242-246, doi:10.1126/science.1225354 (2012).

[2] Prettyman, T. H. *et al.* Extensive water ice within Ceres' aqueously altered regolith: Evidence from nuclear spectroscopy. *Science* **355**, 55-59, doi:10.1126/science.aah6765 (2017).

[3] Yamashita, N. *et al.* Distribution of iron on Vesta. *Meteoritics & Planetary Science* **48**, 2237-2251, doi:10.1111/maps.12139 (2013).

[4] Prettyman, T. H. *et al.* Neutron absorption constraints on the composition of 4 Vesta. *Meteoritics & Planetary Science* **48**, 2211-2236, doi:10.1111/maps.12244 (2013).

[5] Lawrence, D. J. *et al.* Constraints on Vesta's elemental composition: Fast neutron measurements by Dawn's gamma ray and neutron detector. *Meteorit Planet Sci* **48**, 2271-2288, doi:10.1111/maps.12187 (2013).

[6] Peplowski, P. N. *et al.* Compositional variability on the surface of 4 Vesta revealed through GRaND measurements of high-energy gamma rays. *Meteoritics & Planetary Science* **48**, 2252-2270, doi:10.1111/maps.12176 (2013).

[7] Prettyman, T. H. *et al.* Concentrations of potassium and thorium within Vesta's regolith. *Icarus* **259**, 39-52, doi:10.1016/j.icarus.2015.05.035 (2015).

[8] Prettyman, T. H. *et al.* Elemental composition and mineralogy of Vesta and Ceres: Distribution and origins of hydrogen-bearing species. *Icarus* **318**, 42-55, doi:10.1016/j.icarus.2018.04.032 (2019).

[9] Yamashita, N., Prettyman, T. H. & Villarreal, M. N. Catalog of transient radiation events detected by GRaND at Vesta and Ceres. *LPSC XLIX*, #1152 (2018).

[10] Russell, C. T. *et al.* Dawn arrives at Ceres: Exploration of a small, volatile-rich world. *Science* **353**, 1008-1010, doi:10.1126/science.aaf4219 (2016).

[11] Villarreal, M. N. *et al.* The Dependence of the Cerean Exosphere on Solar Energetic Particle Events. *The Astrophysical Journal* **838**, L8, doi:10.3847/2041-8213/aa66cd (2017).

[12] Rousselot, P. *et al.* Search for water outgassing of (1) Ceres near perihelion. *A&A* **628** (2019).

[13] Landis, M. E. *et al.* Water Vapor Contribution to Ceres' Exosphere From Observed Surface Ice and Postulated Ice-Exposing Impacts. *Journal of Geophysical Research: Planets* **124**, 61-75, doi:10.1029/2018JE005780 (2019).

[14] Prettyman, T. H. *et al.* Dawn's GRaND finale: High spatial-resolution elemental measurements reveal and anomaly at Occator crater. *LPS L*, #1356 (2019).

[15] Prettyman, T. H., Englert, P. A. J. & Yamashita, N. Neutron, gamma-ray, and X-ray spectroscopy: Theory and applications in *Remote Compositional Analysis* (eds J. L. Bishop, J. F. Bell, & J. E. Moersch) Ch. 9, 191-238 (Cambridge University Press, 2019).

[16] Prettyman, T. H. *et al.* Dawn's gamma ray and neutron detector. *Space Science Reviews* **163**, 371-459, doi:10.1007/s11214-011-9862-0 (2011).

[17] Prettyman, T. H. Dawn's Gamma Ray and Neutron Detector: Ephemeris, pointing & geometry at Vesta and Ceres *Dawn Gamma Ray and Neutron Detector collection. PDS Small Bodies Node (SBN).* doi:10.26033/dd8n-nq28 (2021).

[18] Prettyman, T. H. Dawn's Gamma Ray and Neutron Detector: Instrument description. *Dawn Gamma Ray and Neutron Detector collection. PDS Small Bodies Node (SBN).* doi:10.26033/p9v5-ce07 (2021).

[19] Prettyman, T. H. Dawn's Gamma Ray and Neutron Detector: Raw data description. *Dawn Gamma Ray and Neutron Detector collection. PDS Small Bodies Node (SBN).* doi:10.26033/1c9p-et44 (2021).

[20] Yamashita, N. & Prettyman, T. H. Dawn's Gamma Ray and Neutron Detector: BGO calibrated data processing. *Dawn Gamma Ray and Neutron Detector collection. PDS Small Bodies Node (SBN).* doi:10.26033/wska-zt48 (2021).

[21] Prettyman, T. H. *Dawn's Gamma Ray and Neutron Detector: Cruise bundle description* (LID: urn:nasa:pds:dawn-grand-cruise:document:dawn_grand_cruise_bundle_description.pdf, 2021).

[22] Prettyman, T. H. & Feldman, W. C. *PDS data processing: Gamma Ray and Neutron Detector* (LID: urn:nasa:pds:dawn-grand-mars:document:dawn_grand_data_processing.pdf, 2013).

[23] Prettyman, T. H. *Dawn's Gamma Ray and Neutron Detector: Mars bundle description* (LID: urn:nasa:pds:dawn-grand-mars:document:dawn_grand_mars_bundle_description.pdf, 2021).

[24] Prettyman, T. H. & Yamashita, N. *Dawn's Gamma Ray and Neutron Detector: Vesta bundle description* (LID: urn:nasa:pds:dawn-grand-vesta:document:dawn_grand_vesta_bundle_description.pdf, 2021).

[25] Prettyman, T. H. & Yamashita, N. *Dawn's Gamma Ray and Neutron Detector: Ceres bundle description* (LID: urn:nasa:pds:dawn-grand-ceres:document:dawn_grand_ceres_bundle_description.pdf, 2021).

[26] Prettyman, T. H. & Pitman, K. M. *Dawn Gamma Ray and Neutron Detector: DC041 Activity Report* (LID: urn:nasa:pds:dawn-grand-cruise:document:dawn_grand_dc041_activity_report.pdf, 2010).

[27] Yu, H.-F. *et al.* The Fermi GBM gamma-ray burst time-resolved spectral catalog: brightest bursts in the first four years. *A&A* **588** (2016).